the plant journal

SEB SOCIETY FOR EXPERIMENTAL BIOLOGY

The Plant Journal (2024) doi: 10.1111/tpj.17204

CRISPR/Cas9-driven double modification of grapevine *MLO6-7* imparts powdery mildew resistance, while editing of *NPR3* augments powdery and downy mildew tolerance

Loredana Moffa[1,†], Giuseppe Mannino[2,†], Ivan Bevilacqua[1,3,†], Giorgio Gambino[4], Irene Perrone[4], Chiara Pagliarani[4], Cinzia Margherita Bertea[2], Alberto Spada[1,3], Anna Narduzzo[1,3], Elisa Zizzamia[1], Riccardo Velasco[1], Walter Chitarra[1,4,*,‡] and Luca Nerva[1,4,*,‡]

[1]*Council for Agricultural Research and Economics – Research Centre for Viticulture and Enology, Via XXVIII Aprile 26, 31015 Conegliano, TV, Italy,*

[2]*Department of Life Sciences and Systems Biology, Plant Physiology Unit, University of Turin, Via Quarello 15/A, 10135 Turin, Italy,*

[3]*Department of Agronomy, Food, Natural resources, Animals and Environment, University of Padova, Via dell'Università 16, 35020 Legnaro, PD, Italy, and*

[4]*Institute for Sustainable Plant Protection, National Research Council, Strada delle Cacce 73, 10135 Torino, Italy*

Received 16 July 2024; revised 27 October 2024; accepted 28 November 2024.

*For correspondence (e-mail luca.nerva@crea.gov.it and walter.chitarra@crea.gov.it).

†These authors equally contributed as first authors.

‡These authors equally contributed as senior authors.

SUMMARY

The implementation of genome editing strategies in grapevine is the easiest way to improve sustainability and resilience while preserving the original genotype. Among others, the *Mildew Locus-O* (*MLO*) genes have already been reported as good candidates to develop powdery mildew-immune plants. A never-explored grapevine target is *NPR3*, a negative regulator of the systemic acquired resistance. We report the exploitation of a cisgenic approach with the Cre-lox recombinase technology to generate grapevine-edited plants with the potential to be transgene-free while preserving their original genetic background. The characterization of three edited lines for each target demonstrated immunity development against *Erysiphe necator* in *MLO6-7*-edited plants. Concomitantly, a significant improvement of resilience, associated with increased leaf thickness and specific biochemical responses, was observed in defective *NPR3* lines against *E. necator* and *Plasmopara viticola*. Transcriptomic analysis revealed that both *MLO6-7* and *NPR3* defective lines modulated their gene expression profiles, pointing to distinct though partially overlapping responses. Furthermore, targeted metabolite analysis highlighted an overaccumulation of stilbenes coupled with an improved oxidative scavenging potential in both editing targets, likely protecting the *MLO6-7* mutants from detrimental pleiotropic effects. Finally, the Cre-loxP approach allowed the recovery of one MLO6-7 edited plant with the complete removal of transgene. Taken together, our achievements provide a comprehensive understanding of the molecular and biochemical adjustments occurring in double *MLO*-defective grape plants. In parallel, the potential of *NPR3* mutants for multiple purposes has been demonstrated, raising new questions on its wide role in orchestrating biotic stress responses.

Keywords: *Vitis vinifera*, *Erysiphe necator*, stilbenes, New Plant Breeding Techniques (NPBTs), *Plasmopara viticola*.

INTRODUCTION

Climate change, due to its detrimental effects on agriculture and consequently on food production and the global economy, stands as one of the greatest challenges of the century (Malhi et al., 2021). It causes significant shifts in temperature, precipitation, and corresponding alterations in soil characteristics, adversely affecting crop performances (Anderson et al., 2020). Furthermore, these changes may exacerbate the proliferation of pests and pathogens, altering their interactions with plants (Singh et al., 2023). To counteract the development of pathogens, numerous agrochemicals are used, even if their excessive

application revealed negative impacts on the environment and human health (Kim et al., 2017). To mitigate pathogen infections and preserve environmental biodiversity and integrity, alternative strategies must be identified. This necessity is driving researchers to explore innovative solutions, including the development of resilient plant varieties through several approaches. Among other techniques, plant breeding, a historically successful method for crop development, has advanced significantly with the advent of New Plant Breeding Techniques (NPBTs) (Giudice et al., 2021).

The identification of candidate genes is the first critical step for the application of NPBTs (Nerva et al., 2023). Indeed, the development of resistant varieties through conventional breeding relies on harnessing resistance (*R*) genes to trigger the plant immune system and act as the primary defense barrier against pathogens. Upon detecting effectors, plants induce the effector-triggered immunity (ETI) pathway that typically results in localized cell death or in a hypersensitive response (Yuan et al., 2021; Zaidi et al., 2018). An alternative approach for developing disease-resilient crops involves susceptibility (*S*) genes, which play a pivotal role in pathogen-induced diseases, facilitating infection and supporting compatibility between a pathogen and its plant host (Zaidi et al., 2018). In contrast to *R* genes, mutation or loss of function of *S*-genes confers resistance to pathogens (van Schie & Takken, 2014). *Mildew Locus-O* (*MLO*) genes are acknowledged *S*-genes, prominently associated with powdery mildew (PM) susceptibility. They were initially characterized in barley (Büschges et al., 1997; Piffanelli et al., 2002), then their role in the regulation of PM susceptibility has been extensively corroborated across a broad spectrum of plant species, including *Arabidopsis* (Consonni et al., 2006, 2010), tomato (Zheng et al., 2013), wheat (Li et al., 2022), apple (Pessina, Angeli, et al., 2016), pea (Humphry et al., 2011), and grapevine (Pessina, Lenzi, et al., 2016; Wan et al., 2020). *MLO* genes encode proteins characterized by a seven-transmembrane domain (including a CaM-binding domain) structure localized on the plasma membrane and acting as Ca^{2+} channels (Gao et al., 2022; Kim et al., 2002; Reddy et al., 2003). The MLO family is divided into seven phylogenetic clades, among these only two encompass *S*-genes: clade IV, housing all monocot *S*-genes, and clade V, containing all dicot *S*-genes (Acevedo-Garcia et al., 2014). While not all members of clades IV and V exhibit *S*-gene features, potential candidates can be discerned during early stages of PM infection due to heightened expression levels. For instance, in grapevine, three out of four clade V-*MLO* genes (*VvMLO7*, *VvMLO11*, and *VvMLO13*) show an early increased expression after PM infection (Goyal et al., 2021). Consequently, exploiting RNA interference, the simultaneous knockdown of the genes *VvMLO7* with *VvMLO6* and *VvMLO11* led to a substantial decrease in PM severity (Pessina, Lenzi, et al., 2016). These findings suggest that the knockdown of *VvMLO7*, in combination with *VvMLO6* and *VvMLO11*, plays a crucial role in enhancing PM resilience, whereas the contribution of *VvMLO13* appears less significant. Recent studies have demonstrated the successful application of CRISPR/Cas9 technology to achieve targeted mutagenesis of *VvMLO3* and *VvMLO4* genes in grapevine (Wan et al., 2020). The edited lines exhibited varying phenotypes: while some displayed normal growth patterns, others showed senescence-like chlorosis and necrosis damages. These observations highlight that pleiotropic effects can arise in MLO-edited lines. Notably, four of the *VvMLO3*-edited lines showed increased resistance to PM, a resistance mechanism based on host cell death, cell wall apposition, and the accumulation of H_2O_2.

Systemic Acquired Resistance (SAR) is a key component of plant immunity (Vlot et al., 2021) and salicylic acid (SA) is the key phytohormone accumulated in tissues upon pathogen infection and orchestrating SAR responses (Peng et al., 2021). The *Nonexpressor of Pathogenesis-Related* (NPR) gene class is a key regulator of SA-mediated signal transduction triggered after SA binding. In *Arabidopsis*, this protein family comprises numerous genes, including *NPR1*, *NPR2*, *NPR3*, and *NPR4*. According to the literature, *NPR1* and *NPR2* positively regulate SA association with WRKY and TGA (TGACG-binding) transcription factors in the nucleus, enhancing the expression of *Pathogenesis-Related* (PR) genes by binding to their promoter sequences (Liu et al., 2020). Many studies in various species, such as *Arabidopsis* (Wang et al., 2020; Wu et al., 2012), periwinkle (Sung et al., 2019), and citrus (Dutt et al., 2015; Gómez-Muñoz et al., 2017), confirmed the pivotal role of *NPR1* in inducing *PR* gene expression and pathogen tolerance. Conversely, *NPR3* and *NPR4*, despite being paralogues of *NPR1*, exhibit an antagonistic role, functioning as transcriptional co-repressors of key immune regulators such as SARD1 and WRKY70, as well as adaptors of Cullin3 (CUL3)-based E3 ligase, which mediates the degradation of NPR1 (Chang et al., 2019; Liu et al., 2020). This opposite role was demonstrated in previous experiments performed on *Theobroma cacao* in which the knock-out of *TcNPR3* resulted in enhanced resilience to *Phytophthora capsici* and *Phytophthora tropicalis*, accompanied by elevated expression of downstream defense genes (Fister et al., 2018; Shi et al., 2013). We chose a similar approach in grapevine with the aim of reducing the susceptibility against different fungal pathogens. A similar approach in grapevine would potentially allow reducing susceptibility against not only PM but also *Plasmopara viticola*, the causative agent of downy mildew (DM).

CRISPR/Cas9 stands out among the NPBTs as a powerful and precise tool, which can be used to enhance tolerance to biotic and abiotic stresses in plants and also to functionally characterize putative genes involved in plant immunity and environmental adaptation (Giudice et al., 2021; Zhu et al., 2020). Despite the global economic significance of grapevines, there are currently few studies on CRISPR/Cas9-mediated genome editing (Li et al., 2020; Scintilla et al., 2022; Wan et al., 2020). This is due to a long and challenging process that encompasses many difficult steps, like the necessity to develop embryogenic calli, the recalcitrance of such tissue to regenerate embryos and the following regeneration of plants from the developed embryos (Nuzzo et al., 2022). Furthermore, the difficulties in developing marker-free edited grape plants limit the application of genome editing. Indeed, conventional transformation approaches based on *Agrobacterium* spp. rely on the presence of foreign genes (i.e., the Cas9 protein, the gRNAs, and the selection marker), which then turn the plants into genetically modified organisms (GMOs) (Nerva et al., 2023). As such, GMOs undergo specific regulations (very restrictive in Europe) and meet resistance from both the society and politicians (Ceasar & Ignacimuthu, 2023). For this reason, the exploitation of transgene-free approaches is the only way to avoid the GMOs regulation and to develop marketable products. In such context the exploitation of DNA-free genome editing (Gambino et al., 2024) or the cisgenic-like approach (Nerva et al., 2023) is the only two available strategies for preserving the original genotype avoiding the generation of GMOs. In specific, the cisgenic-like approach relies on the exploitation of recombinase systems able to remove the transgenes once the editing event is achieved (Dalla Costa et al., 2016; Ye et al., 2023). Among the different recombinase systems, the Cre/loxP recombination system has been extensively documented for its use in eliminating selectable marker genes across various species (Gilbertson, 2003; Ye et al., 2023). The expression of Cre recombinase can be controlled by inducible promoters that respond to heat, cold, drought, or chemical stimuli (Éva et al., 2018; Khattri et al., 2011; Wang et al., 2005; Zuo et al., 2001).

This study reports an efficient approach to overcome these difficulties and provides novel insights into the biological function of genes involved in pathogen-resilience through application of the CRISPR/Cas9 technique. Notably, knock-out grapevine plants with double mutation of *VvMLO6* and *VvMLO7* and *VvNPR3* mutants exhibited significantly enhanced tolerance against PM, with the double mutants resulting almost immune. Interestingly, only NPR3 mutants exhibited also an improved resilience against downy mildew (DM), disease caused by the fungal pathogen *P. viticola*. Finally, the Cre-loxP system for transgene excision displayed a good efficiency in reducing the copy number and allowed to recover a MLO6-7 edited plant without the presence of transgenes.

RESULTS

Cre-lox recombinase system allows the transgene copy number to be lowered up to ten times

Phylogenetic placement of VvMLO6 and VvMLO7 protein sequences confirmed their belonging to MLO Clade V (Figure S1). Similarly, the VvNPR3 protein grouped within the clade of NPR3/4 from *Arabidopsis* and very close to NPR3 from *T. cacao* (Figure S2). Employing a conventional *Agrobacterium*-mediated transformation protocol, we induced the differentiation of somatic embryos of *Vitis vinifera* cv Chardonnay and 18 putatively transgenic embryos were obtained. We successfully regenerated 17 plants harboring the *MLO6/MLO7* silencing construct, all of which exhibited amplification with Cas9 primers. Evaluation of editing efficiency was assessed on PCR amplicons using TIDE software, revealing successful events in 13 (out of 15) of the selected plants. Concurrently, for the *NPR3* construct, 129 somatic embryos of "Chardonnay" were obtained after *Agrobacterium*-mediated transformation. Forty-eight plants were regenerated from embryos, 53 of which exhibited successful transformation (positive to Cas9) and 33 displayed targeted editing. Subsequent screening of the target regions of gRNAs VvNPR3g2, VvMLO6g7, and VvMLO7g25 via high-throughput sequencing unveiled some editing frequencies exceeding 90% (Figure 1). Three lines for each construct were selected (editing characteristics of each line are reported in Figure 1) and subsequently exploited for further analyses. Specifically, for NPR3g2, the lines NPR3#4, NPR3#9, NPR3#15 exhibited editing frequencies of 88.71, 89.82, and 90.35% respectively (Figure 1E). Regarding mutations in the *MLO* genes, the percentage of modified reads around VvMLO6g7 was consistently higher than 85% across all lines (Figure 1A). A larger variation in editing frequencies was observed for MLO7g25, as illustrated in Figure 1(C). The mutations associated with the lines selected for further analyses and experiments are illustrated in Figure 1(B,D,F). Off-target analysis using Sanger sequencing revealed that exclusively the target sequence has been mutated for each gRNA. After confirming successful genome editing, selected edited lines (MLO#1, #3, #9 and NPR#4, #9, #15) and wild-type (WT) plants underwent micropropagation and acclimatization (25 plants for each) for further analysis. No phenotypic differences of *MLO6-7*- and *NPR3*-edited lines in comparison with WT have been observed (representative plants are shown in Figure S3).

Edited plants were subjected to high temperature in order to activate the excision Cre-loxP system. To evaluate the copy number variation (CNV) in acclimatized plants of *NPR3*- and *MLO6/7*-edited lines compared to the original regenerated ones (still *in vitro*), qPCR was performed on at least 10 plants for each line. Interestingly, following the heat treatments, some plants displayed a copy number up

(A)

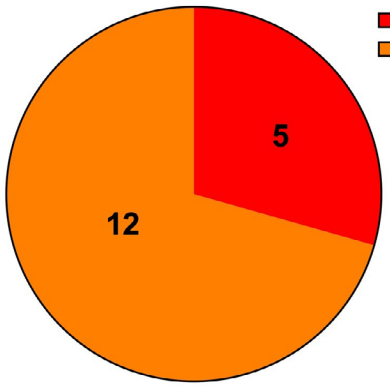

MLO6g7

(B)

MLO6g7		Mutation	%	Mutation	%
#1	Homozygous	-CC	86,79		
#3	Heterozygous	+A	42,14	-C	37,48
#9	Homozygous	-C	84,93		

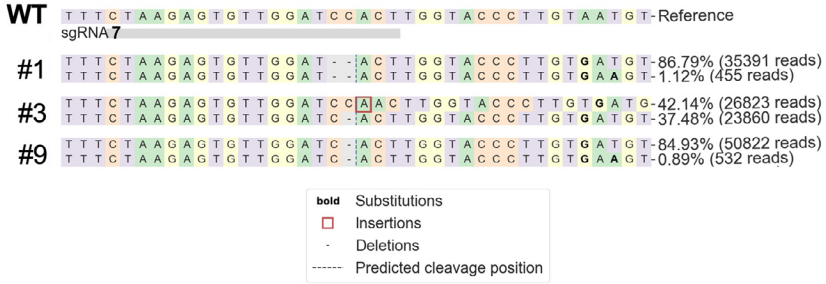

(C)

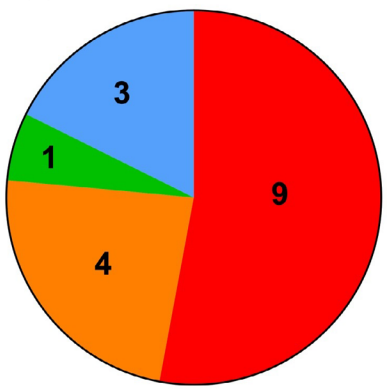

MLO7g25

(D)

MLO7g25		Mutation	%	Mutation	%
#1	Heterozygous	+T	43,57	+A	41,35
#3	Heterozygous	-9 bp	47,79	+A	41,93
#9	Heterozygous	-9 bp	47,17	+A	39,74

(E)

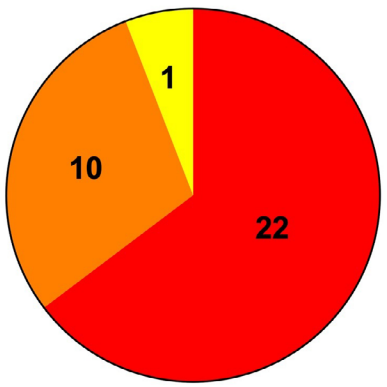

NPR3g2

(F)

NPR3g2		Mutation	%	Mutation	%
#4	Homozygous	+A	88,71		
#9	Heterozygous	-TAAT	48,32	+AA	41,50
#15	Heterozygous	-37 bp	72,04	-14 bp	18,31

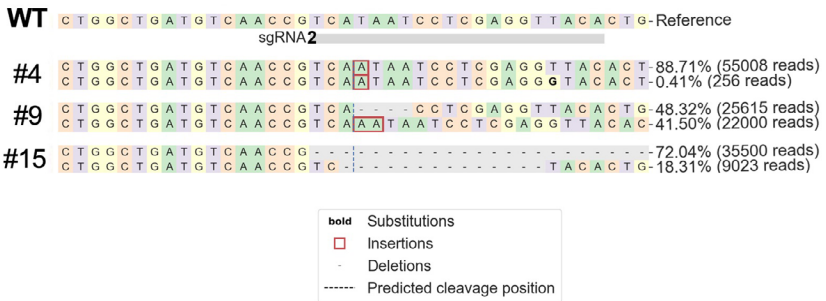

Figure 1. Alignment and editing frequencies.
(A, C, E) Frequencies of editing percentages for each guide RNA (gRNA) and target gene. Numbers within the pie charts represent the number of plants belonging to the specific class.
(B, D, F) For each target gene, three lines have been selected for subsequent experiments. The editing event for each line is reported for MLO6g7 (B), MLO7g25 (D), and NPR3g2 (F).

Table 1 Copy number variation (CNV)

Target—*VvMLO6* and *VvMLO7*				Target—*NPR3-like*			
Line	Plant	CN	Reduction (%)	Line	Plant	CN	Reduction (%)
MLO6-7#1		1.0		NPR3#4		1.7	
	1	0.4	60		1	0.4	71
	2	0.4	60		2	0.6	57
	3	0.3	70		3	0.5	64
	4	0.3	70		4	0.3	79
	5	0.3	70		5	0.4	71
	6	0.5	46		6	0.4	71
	7	0.3	66		7	0.5	64
	8	0.6	40		8	0.4	71
	9	0.6	44		9	0.4	71
	10	0.6	41		10	0.4	71
	11	0.4	60		11	0.6	57
	12	0.3	70		12	0.3	79
	13	0.3	70		13	0.3	79
MLO6-7#3		1.0		NPR3#9		2.0	
	1	0.2	80		1	0.4	77
	2	0.1	90		2	0.4	77
	3	0.3	70		3	0.5	71
	4	0.1	90		4	0.3	82
	5	0.1	90		5	0.5	71
	6	0.2	80		6	1.7	4
	7	0.2	80		7	1.6	8
	8	0.1	90		8	1.6	8
	9	0.1	90		9	1.1	35
	10	0.1	90		10	1.0	41
	11	0.2	80		11	1.1	35
	12	0.1	90		12	1.1	35
	13	0.0	100		13	1.3	23
MLO6-7#9		1.0		NPR3#15		1.4	
	1	0.4	60		1	0.2	90
	2	0.4	60		2	0.5	75
	3	0.5	50		3	0.6	72
	4	0.3	70		4	0.5	73
	5	0.4	60		5	0.6	72
	6	0.5	50		6	0.4	80
	7	0.5	50		7	0.6	70
	8	0.6	40		8	0.5	75
	9	0.4	60		9	2.0	0
	10	0.4	60		10	0.3	85
	11	0.5	50		11	0.3	85
	12	0.4	60		12	0.4	80
	13	0.5	50		13	0.3	85

Plants subjected to heat treatments were analyzed to determine the final copy number and relative percentage reduction. CN, copy number. The original copy number is reported beside the line name.

to 10 times lower than the original plant from which they derived (Table 1). Later in the season, once the plants were acclimatized, the CNV was checked again, and one MLO6-7#3 plant resulted with a copy number of 0. To further confirm the absence of transgene PCR reactions at 35, 40, and 45 cycles have been run (Figure S4). The plant was checked again with the Sanger sequencing method and the editing status was confirmed.

Edited plants displayed from increased tolerance to immunity to *Erysiphe necator*, depending on the edited target

Initial signs of spontaneous PM infection were observed in WT plants at the end of August 2023 (Figure 2). When all WT plants exhibited symptoms on at least three leaves, disease indices were assessed. WT plants displayed the highest susceptibility to PM, with an incidence of 84% and a severity of 13% (Figure 2A,B). In contrast, the edited lines, particularly the *MLO*-edited ones, showed significantly reduced infection rates. Specifically, the MLO6-7#1, MLO6-7#3, and MLO6-7#9 lines exhibited markedly lower incidences of 0.5, 0, and 4.5%, respectively, all statistically different from the WT (Figure 2A). Correspondingly, these MLO-edited lines demonstrated significantly lower disease severities, ranging from 0 to 0.2% (Figure 2B). Similarly, the *NPR3*-edited lines also exhibited reduced infection, though to a lesser extent than the MLO-edited lines. Notably, NPR3#4 and NPR3#9 lines showed a significantly lower incidence than the WT, while NPR3#15 showed an incidence of 75.3%, not significantly different from the WT plants (Figure 2A). However, all *NPR3*-edited lines displayed significantly lower severities of 3.1, 1.7, and 6.7%, respectively, compared to the WT plants (Figure 2B). Representative examples of leaf infections are reported in Figure 2(C–E).

Evaluation of leaf ecophysiological parameters, including measurement of the chlorophyll content index (CCI), maximum quantum efficiency of photosystem II by determination of the F_v/F_m ratio and leaf thickness, was conducted for both WT and edited plants (Figure 2F–H). CCI analysis (Figure 2F) indicated a slightly lower, though not statistically significant, value in *NPR3* edited lines in comparison with both WT and *MLO6-7* mutated plants. F_v/F_m values did not significantly vary across edited and WT plants (Figure 2G), likely suggesting that PSII efficiency was not altered. Conversely, leaf thickness showed a significant increase only in *NPR3* edited plants, while no significant differences were recorded between MLO6-7 edited lines and WT plants (Figure 2H).

Only NPR3-edited plants displayed increased tolerance to *Plasmopara viticola*

Considering the improved resilience observed while the spontaneous infection of PM was occurring, a controlled experiment using DM was initiated during the summer 2024. Once confirmed that the non-inoculated leaves did not show any sign of infection after 7 days of incubation, we proceeded to evaluate the inoculated leaves following the OIV descriptor 452-1. The experiment was repeated twice in order to confirm the results with two independent replications. Results showed that WT- and MLO-edited lines displayed a similar distribution across the disease resistance classes in both experiments (Figure 3A,B). In fact, widespread visible signs of infection were observed both in WT and MLO-edited lines by the emergence of *P. viticola* from the abaxial surface of the leaves (Figure 3C). On the contrary, both the independent replication confirmed a higher disease resistance score for the *NPR3*-edited lines (Figure 3A,B), with a highly significant difference from the WT (*P*-value <0.01). In fact, only mild signs of infection were observed with small and localized emergence of DM (Figure 3C).

Leaf-associated fungal community composition is influenced by the edited target

To further confirm the results obtained with the visual scoring of PM incidence and severity we also evaluated the presence of *Erysiphe* in terms of relative abundance through the ITS metabarcoding (Figure 4). Regardless of whether the single edited lines (Table S1) or the editing targets (averaging the three independent lines) (Table S2) were evaluated, the relative abundance of *Erysiphe* was consistently lower in the mutagenized plants. Furthermore, the sequencing results confirmed a stronger inhibition of *Erysiphe* in *VvMLO6* and *VvMLO7* edited lines, which displayed an average log2 fold-change (FC) of −3.65 (*P*-value 0) when compared to the WT (Figure 4; Table S2). Similarly, a significant reduction in *Erysiphe* relative abundance was also observed in *VvNPR3* edited lines but to a lesser extent (average FC of −0.72) (Figure 4; Table S2).

Looking at the whole fungal community responses, both types of editing (i.e., *VvMLO6-7* or *NPR3*) modify fungal taxa abundances. For each editing event, a total of 126 taxa displayed significant differences in at least one line (Table S1). More in detail, when considering the target gene as the variable, only 49 taxa still display a significant difference when comparing *VvMLO6-7* or *NPR3* mutated lines against the WT (Table S2). When we consider the latter, we can see that some modifications are shared, like, for example, the significantly lower abundance of *Hannaella* (FC of −2.65 and −2.85 in *VvMLO6-7*-edited and *NPR3*-edited plants, respectively) and *Rhodotorula* (FC of −3.35 and −4.21 in *VvMLO6-7*-edited and *NPR3*-edited plants, respectively) genera, between both editing targets (Table S2). Other shifts in the fungal community are instead exclusively related to a single type of modification, like, for example, a significantly lower abundance of amplicon sequence variants (ASV) assigned to *Dactylonectria*, *Ilyonectria*, and *Pleosporales incertae sedis* genera (FC −0.21, −0.36 and −2.55, respectively) which was observed only in the *NPR3* edited lines (Table S2). Conversely, a higher abundance of *Chaetomium* and *Colletotrichum* (FC 2.32 and 1.68, respectively) was observed on the leaves of *VvMLO6-7*-edited plants (Table S2) (Fan et al., 2023; Hassan et al., 2022). Finally, it is worth noting that the relative abundance of the *Ampelomyces* genus is stable in the

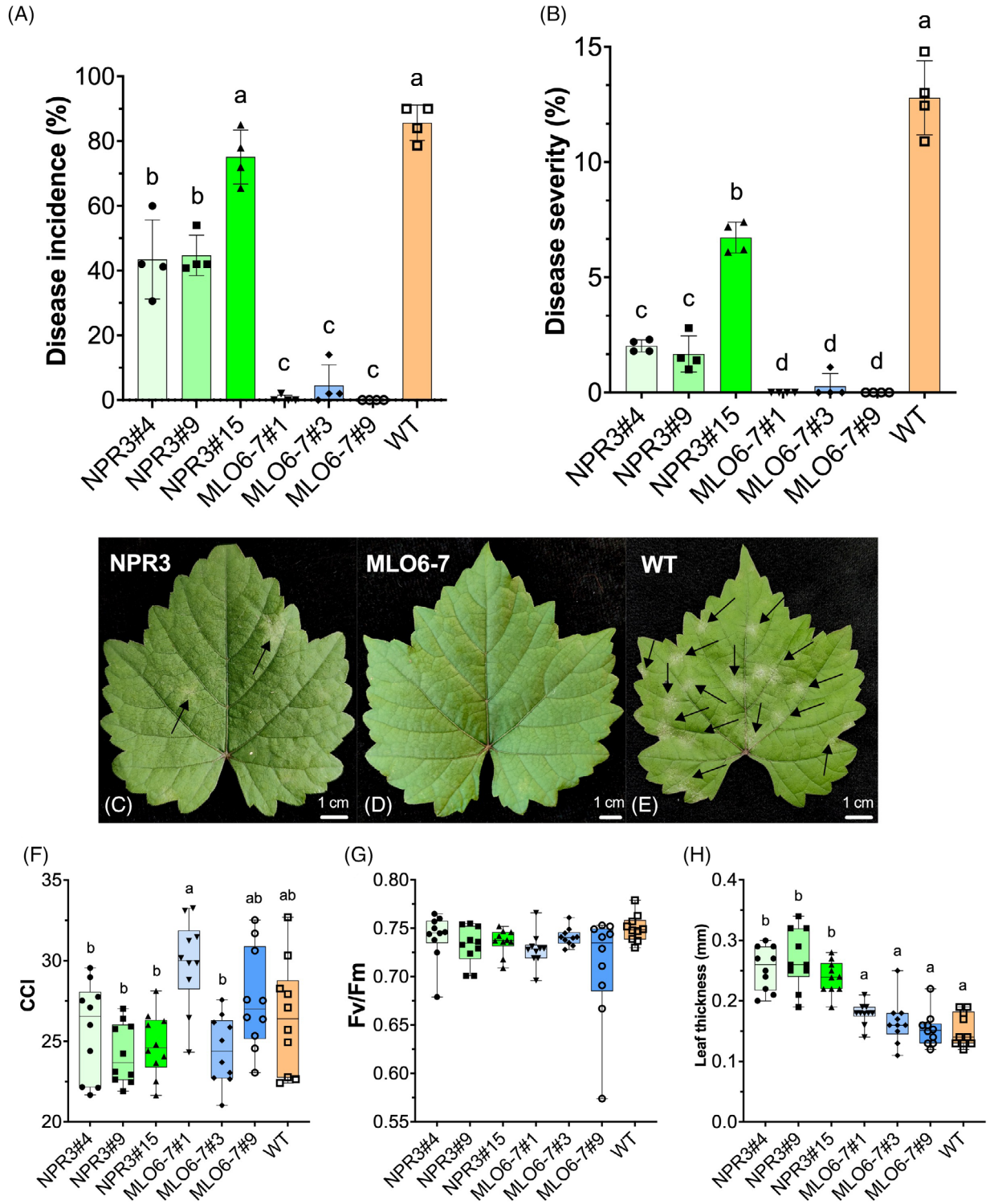

Figure 2. Evaluation of powdery mildew infection and leaf ecophysiological traits.
Disease indices of powdery mildew-infected plants were collected through the grape assess mobile application.
(A, B) (A) Incidence and (B) severity percentages of leaf infections (n = 4, each biological replicate is composed by at least 50 observations).
(C–E) Representative leaf of *NPR3*-edited, *MLO6-7*-edited and WT-plants, respectively. Black arrows indicate sites of infection.
(F–H) Leaf ecophysiological traits, including: (F) Chlorophyll Content Index (CCI) (n = 10), (G) maximum quantum efficiency of PSII (F_v/F_m) (n = 10) and (H) leaf thickness (n = 10) were collected using a PhotosynQ apparatus. Lowercase letters above bars indicate significant differences among the samples, as determined by ANOVA followed by Tukey post hoc test. All data in bar charts represent mean values ± standard deviation bars. In box-plot charts, box limits indicate the range of the central 50% of the data, with a central line marking the median value and lines extend from each box to capture the range of the remaining data.

The Plant Journal published by Society for Experimental Biology and John Wiley & Sons Ltd.,
The Plant Journal, (2024), doi: 10.1111/tpj.17204

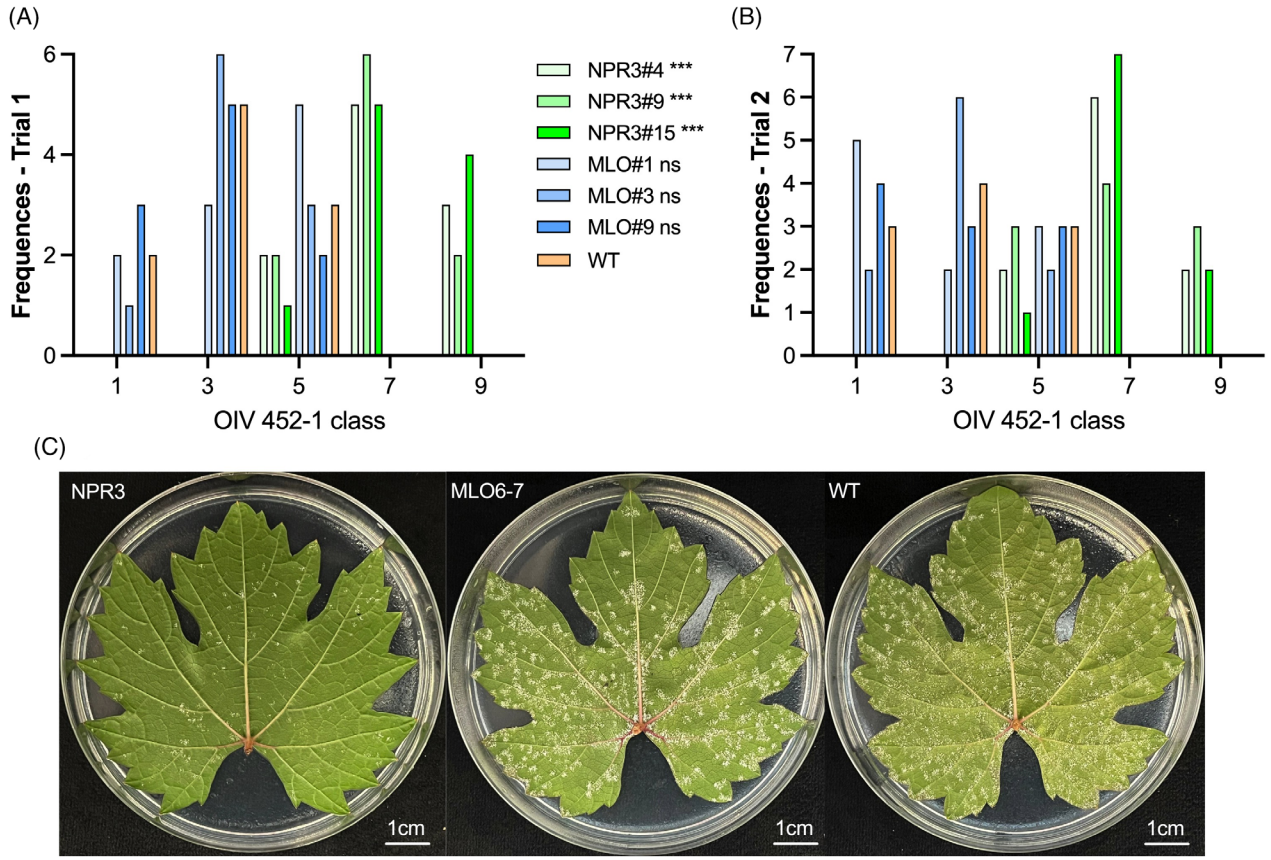

Figure 3. Evaluation of downy mildew infection.
Assessment of leaf resistance to *Plasmopara viticola* using the OIV 452-1 descriptors (the higher the value, the higher the resistance).
(A, B) Distribution of class frequencies recorded during the first trial 1 (A) and trial 2 (B) (n = 10 for each trial). The two trials were carried out 15 days one from the other. Asterisks (***) aside the legend denote highly significant differences as attested by the chi-squared test on the class frequencies (P-value ≤0.001).
(C) representative leaf of *NPR3*-edited, *MLO6-7*-edited and WT-plants, respectively.

NPR3 edited lines while it is significantly lower in *VvMLO6-7* edited ones (Table S2).

Leaf molecular responses of VvMLO6-7 and NPR3-edited plants are partially overlapping

To understand the systemic responses resulting from editing events and pathogen attack, we collected leaves from plants infected by *E. necator* 7 days after the appearance of the first symptoms. The leaves were then used to profile transcriptome reprogramming events through RNA-seq.

Looking at the *MLO6-7* edited lines, 376 genes were significantly differentially regulated (FC >1) in comparison with the WT plants (Table S3). The majority of the genes (211 over 376) show downregulation, with an overrepresentation of genes belonging to the energy metabolism cluster, photosynthesis, and transport (Figure S5A–C). Instead, all the *MLO6-7* edited lines displayed an upregulation of genes belonging to the carbohydrate metabolism (Figure S5A–C).

When considering the *NPR3-like* edited lines, the number of significantly differentially regulated genes (FC >1) in comparison with WT plants was 1216 (Table S4). Contrary to what was observed in *MLO6-7* edited plants, a slight majority of genes were upregulated (646 over 1216). Among them we observed an overrepresentation of genes belonging to the metabolic process cluster (including three polyphenol oxidases—VIT_00s0480g00060, VIT_00s0480g00070, VIT_10s0116g00560), particularly those involved in maltose, starch, polysaccharide and thiamine-containing compound metabolism (Figure S6D–F). Similarly, *NPR3-like* edited lines displayed a downregulation of genes belonging to energy metabolism, photosynthesis, and transport (Figure S5D–F). Genes belonging to the alpha-expansin group (VIT_17s0053g00990, VIT_06s0004g07970, VIT_14s0108g01020, VIT_13s0067g02930) as well as auxin-responsive genes (VIT_03s0038g01120, VIT_03s0038g00950, VIT_05s0062g00850, VIT_11s0016g00640) were strongly downregulated. Interestingly, two isoforms of *MLO* genes (namely *MLO1* and *MLO7*) were downregulated in *NPR3*-edited plants (Table S4).

Finally, a comparison between *MLO6-7* and *NPR3-like* edited lines revealed 153 genes with a significant

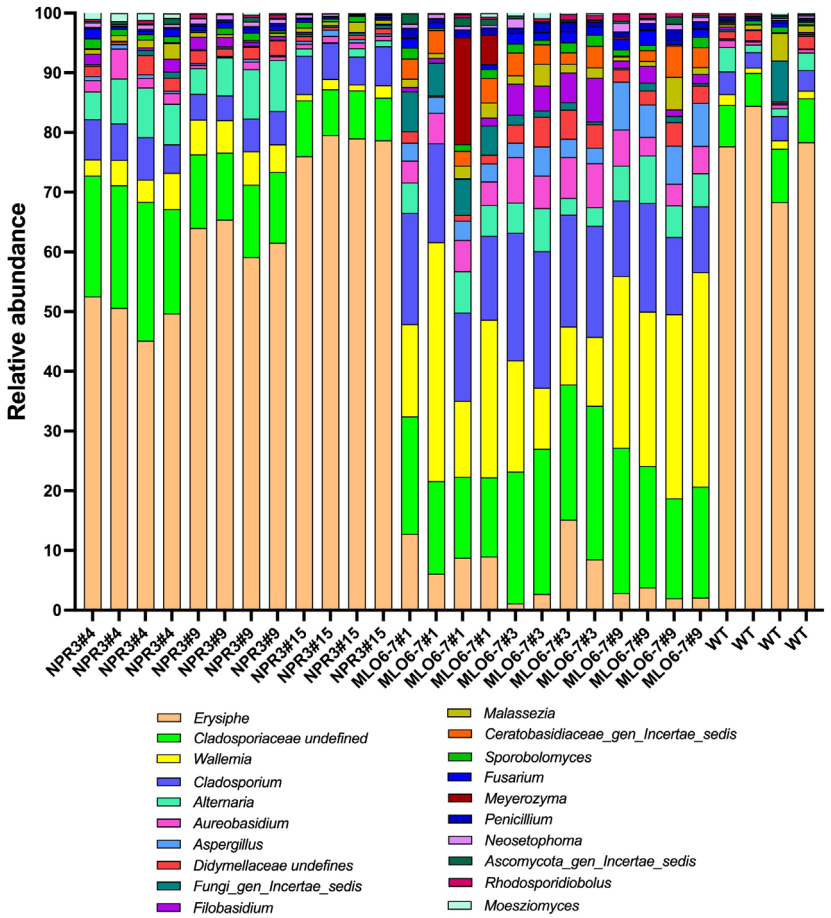

Figure 4. Analysis of the leaf-associated fungal population in edited and WT plants.
Fungal genera were identified through the qiime2-ITSexpress pipeline and compared among samples ($n = 4$). Only the top 20 representative genera among the total classified amplicons were retained in the graphic representation.

differential expression pattern between the two conditions (Table S5). Among them, 62 displayed exclusively downregulation, while 91 displayed a stronger upregulation in *MLO6-7*-edited compared to *NPR3*-edited plants. Looking at the processes downregulated in *MLO6-7*-edited lines, an enrichment of genes involved in transport (e.g., anion transport and inorganic anion transport) and response to abiotic stimuli (e.g., spermine and polyol metabolism) was observed (Figure S5G–I). In parallel, an upregulation of genes related to peculiar processes in *MLO6-7*-edited lines was observed, specifically those involved in maltose and starch metabolism and cell homeostasis (iron homeostasis and RNA/mRNA modification) (Figure S5G–I).

Stilbenes are differentially accumulated in MLO6/7 and NPR3-edited plants

In order to assess alterations in key target defense-related metabolites (i.e., stilbenes), HPLC-DAD-MS/MS analysis was conducted on edited MLO and NPR lines compared with WT plants. HPLC-MS/MS analyses revealed the presence of *t*-resveratrol (Figure 5A) and its glycosylated form (piceid) (Figure 5B), along with two different oxodimers of resveratrol (δ-viniferin and ε-viniferin) (Figure 5C,D). Looking at the whole dataset, our values were similar to those measured in the leaves of different grape cultivars (Mohammadparast et al., 2024). As a general trend, the lowest levels were found in WT conditions, while the *MLO6-7* and *NPR3* mutant lines exhibited slightly higher contents. On average, the leaves of plants mutated for these genes showed an increase in total stilbene content compared to the WT (Figure 5A), of +1.87 and +1.60, respectively. Specifically, while the rise in *t*-resveratrol content was similar between *MLO6-7* and *NPR3* plants (about +1.4), edited lines resulted in different profiles for the more complex forms of stilbenes. Specifically, the *MLO6-7* mutant plants showed a substantial increase in the polymeric forms of *t*-resveratrol, with increments of +2.3 and +1.73 for δ-viniferin and ε-viniferin (Figure 5C,D), respectively. Instead, the *NPR3* mutant plants, despite an increase in δ-viniferin (+1.91), exhibited a significant increase in piceid, with an increment of +1.65 (+1.71) (Figure 5B).

To comprehensively analyze the oxidative profile of WT, *MLO6-7*, and *NPR3* leaves, the total peroxide content (Figure S7A), total polyphenol content (Figure S7B), and the enzymatic activity of superoxide dismutase (SOD) and catalase (CAT) (Figure S7C,D) were determined. Under our experimental conditions, a significant reduction in total peroxide content was observed in the mutated lines.

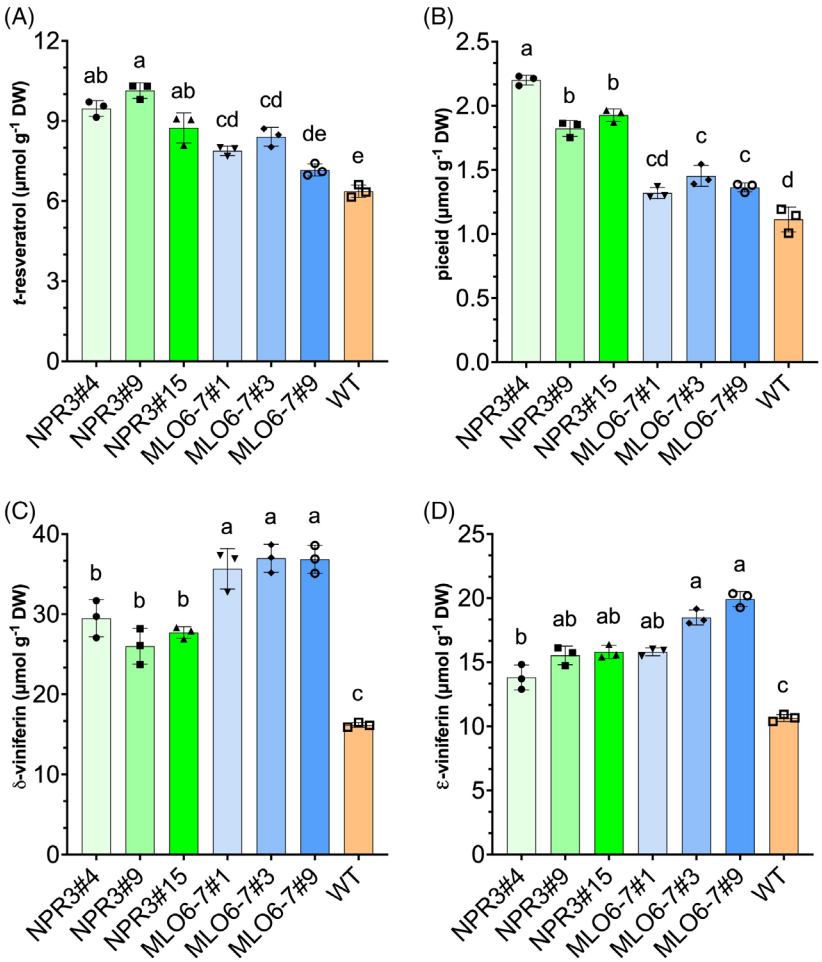

Figure 5. Quantification of leaf stilbenes in edited and WT plants.
(A–D) Contents of trans-resveratrol (A), piceid (B), δ-viniferin (C), and ε-viniferin (D) quantified in leaf samples of *Vitis vinifera* wild type (WT), MLO6-7-edited, or NPR3-like plants ($n = 3$ for each line and compound). Data are expressed as µmol g^{-1} of dry weight (DW). Lowercase letters above bars indicate significant differences among the samples, as determined by ANOVA followed by Tukey post hoc test. All data in bar charts represent mean values ± standard deviation bars.

Specifically, values decreased from 1.55 ± 0.22 µmol of H_2O_2 to approximately 1.04 ± 0.09 and 0.89 ± 0.05, for *MLO6-7* and *NPR3* plants, respectively (Figure S3A). In contrast, a complementary trend was observed for the total polyphenol content (TPC) measured through the molybdenum and tungsten salt reduction assay (Figure S7B). TPC ranged from 165.80 ± 10.5 (WT) to 446.46 ± 19.22 (NPR3#9). Although variations were evident among the mutated plant lines, WT plants exhibited a significantly lower polyphenol content, approximately −2.05 (in comparison with *MLO6-7*) and −2.55 (in comparison with *NPR3*) times lower. From the enzymatic point of view, both SOD and CAT activities were significantly reduced in WT plants compared to the edited lines (Figure S7C,D). However, while SOD appeared to be more active in the *MLO6-7* edited lines (Figure S7C), the *NPR3* lines exhibited higher CAT levels (approximately +2.05) compared to WT (Figure S7D).

DISCUSSION

The development of gene-edited plant varieties able to cope with environmental stresses represents a promising tool to improve agricultural sustainability (Giudice et al., 2021). Considering the specific case of grapevine, implementing genome editing strategies emerges as the most straightforward method for enhancing sustainability and resilience while maintaining the original genotype (Giudice et al., 2021). Gene editing allows to disrupt as little as possible the genome architecture and the gene pool of "elite" varieties while improving their stress resilience features (Sheridan, 2024).

Despite the great potential of genome editing, its application in grapevine is still limited, mainly due to three bottlenecks. The first issue is related to the knowledge of gene functions. Even though the grapevine genome has been available for about 20 years (Jaillon et al., 2007; Velasco et al., 2007; Wang et al., 2024) most genes are still annotated only *in-silico*, limiting the available pool of targets (Nerva et al., 2023). A second limitation concerns the development of embryogenic calli, the explant required as a starting point to perform either *Agrobacterium*-mediated transformation or DNA-free transfection of protoplasts (Gambino et al., 2024; Najafi et al., 2023; Scintilla et al., 2022; Tricoli & Debernardi, 2024). The last limitation,

but equally important, is the ability of the calli to regenerate (Nuzzo et al., 2022). The latter two limitations are primarily associated with genetic features, meaning that each specific variety possesses its own ability to produce embryogenic calli and its own regeneration efficiency (Gribaudo et al., 2017; Nuzzo et al., 2022). Collectively, these limitations led to the application of editing approaches predominantly in easy-to-work genotypes, like, for example, table grape varieties [e.g., Crimson seedless or Sugraone (Clemens et al., 2022; Scintilla et al., 2022)] or raisin grapes [e.g., Thompson seedless (Najafi et al., 2023; Olivares et al., 2021)], which represent only a small area of cultivated lands. A few examples of gene editing in elite wine grape cultivars are beginning to emerge in the literature (Gambino et al., 2024; Tricoli & Debernardi, 2024), and here we report its application in the worldwide cultivated Chardonnay cultivar.

To preserve the original genetic background and avoid the issues related to DNA-free or stable transformation approaches (Nerva et al., 2023), we decided to exploit a recombinase mechanism based on the Cre-loxP system (Chong-Pérez et al., 2012; Gilbertson, 2003). The recovered data showed that we reduced the transgene copy number by 90%, applying a single cycle of heat-shock, and that lately in the season a complete transgene removal was achieved at least in one MLO6-7#3 plant. This result is in contrast to what previously observed in grapevine using flp-frt recombination, which did not result in a significant reduction of copy number in transgenic grape plants (Dalla Costa et al., 2020), suggesting a more efficient activity of the Cre-loxP system. This result is very encouraging since, as previously mentioned, the editing of grapevine protoplasts, and the subsequent regeneration of plants, is still very challenging. Thus, by avoiding such a step we will be able to improve the number of exploitable genotypes while reducing the time for generation of edited grapevine plants.

Considering the limited gene function information, we opted to exploit already available information on *VvMLO6* and *VvMLO7* to investigate the effects of a double mutation. Indeed, previous studies took into consideration the role of the different *MLO* genes in grapevine (Feechan et al., 2008) confirming that *MLO6* and *MLO7* were the two most promising targets (Pessina, Angeli, et al., 2016). Our results highlight that the double mutation led to the almost complete loss of susceptibility to PM. Indeed, both disease indices (incidence and severity) remained close to zero, with just one *MLO6-7*-edited line showing very mild infection symptoms. It is worth noting that, even if *MLO* mutants were already generated in transgenic grapevines using RNA interference (Pessina, Lenzi, et al., 2016), no studies have looked at the metabolic shift induced by the disruption of these genes. Indeed, the understanding that mutations in *MLOs* can elicit broader effects beyond conferring resistance to PM has long been reported (Wolter et al., 1993). In particular, *MLO* mutants of herbaceous species present a premature decay of photosynthesis associated with early decline in photosynthetic performance, an altered transcriptional profile, and abnormal levels of secondary metabolites derived by tryptophan (Consonni et al., 2010). All these modifications led to spontaneous mesophyll cell death, probably reflecting an uncontrolled senescence program (Piffanelli et al., 2002). Additionally, a recent work conducted on *Arabidopsis* linked the emergence of pleiotropic effects to the nitrogen deficiency, pointing out that also external factors can alter the establishment of deleterious effects (Freh et al., 2024). Our findings show that grapevine mutants for *MLO6* and *MLO7* display a decline of molecular processes related to photosynthesis process, partially overlapping to what was observed in *Arabidopsis* (Consonni et al., 2010). Nonetheless, *MLO* grape mutants displayed a transcriptional reprogramming of genes involved in carbohydrate metabolism, a response usually linked to plant immunity (Trouvelot et al., 2014), suggesting a possible trade-off toward growth-defense. Additionally, the biochemical profiling revealed an overaccumulation of stilbenes, which have been consistently identified as primary defense responses to pathogen attacks (including PM) (Schnee et al., 2008), and largely recognized as markers for disease resistance in grape plants (Viret et al., 2018). Collectively, these findings suggest that also in grapevine *MLO* mutants, as in other species where *MLOs* were studied, an enhancement of some defense responses was established, at least considering changes in the stilbene profile. Further investigation on this subject is definitely needed to better elucidate the whole metabolomics changes controlling such defensive mechanisms.

In parallel to mutations of *MLOs*, we decided to explore the effects of the loss of function mutants of *NPR3-like*. This gene belongs to the plant-conserved Nonexpresser of Pathogenesis-Related (NPR) protein family and is classified within clade II, which, together with members of clade I, plays prominent roles in orchestrating plant defense responses (Zhou et al., 2023). Their activity is mediated by the ability to bind salicylic acid, but with an opposite outcome. While members of clade I are essential for activating the SAR responses (Glazebrook et al., 1996), members of clade II impair the activation of defense responses (Ding et al., 2018). In fact, loss of function mutants for *NRP3* and *NPR4* in *Arabidopsis* showed an increased activation of the immune system and a concomitant upregulation of PR proteins, leading to an increased tolerance to pathogen attacks (Fu et al., 2012). Similarly, the transient knock-out of *NPR3* in *T. cacao* leaves limited the spread of *P. tropicalis* (Fister et al., 2018). Considering this information, and that in grapevine there is only one member of clade I (*VvNPR1*) (Le Henanff et al., 2009) and

one member of clade II (*NPR3*) (Zhou et al., 2023), we opted to evaluate an editing approach targeting the *NPR3* gene. From the susceptibility point of view, the *NPR3*-edited lines displayed a significant improvement in terms of resilience against PM but to a lesser extent if compared to *MLO* mutants. In fact, based on disease incidence, only two out of three *NPR3-like* mutant lines (*i.e.*, NPR3#4 and NPR3#9) displayed a significant difference when compared to WT plants. Conversely, the disease severity index was always significantly lower than in WT. These findings are in line with our expectations since in *MLO*-edited plants we disrupted the production of proteins involved in recognition between the fungus and its host, thereby inhibiting fungal growth and tissues colonization. On the other hand, in edited *NPR3-like* plants, we blocked the production of a protein that negatively regulates the plant's defense responses, but which is not involved in the early interaction stages between the pathogen and its host. Nonetheless, a significant downregulation of *MLO1* and *MLO7* was observed, suggesting that NPR3 downregulation can indirectly impair the transcription of *MLO* genes. The exploitation of a pathogen-independent defense mechanism allowed the *NPR3*-edited lines to show, besides improved tolerance to PM, an improved resilience against *P. viticola*, strongly suggesting a much wider resilience to biotic stresses. This feature makes this approach more suitable for generating a broad-spectrum disease tolerance, as also suggested by the metabarcoding analyses which highlighted a significant reduction in the relative abundance of potential pathogens. In addition to the reported molecular and biochemical adjustments, we observed an improvement in leaf thickness probably related to the molecular adjustment (i.e., downregulation of genes encoding alpha-expansins and auxin-responsive factors) involving more complex metabolic processes. Such a trait was already associated with disease tolerance in other species, including woody plants such as *Populus* clones, where those with greater leaf thickness were more tolerant to rust infections (Fernàndez-Martínez et al., 2013). For the first time in genome editing studies, we demonstrated here that the outcomes of a lower infection rate can be confirmed by ITS metabarcoding. Indeed, this approach highlighted a significantly lower presence of *E. necator* on the leaves of both *NPR3-like* and *MLO*-edited plants. In parallel, the relative abundance of *Ampelomyces* was reduced in the *MLO6/7* mutants but not in *NPR3*-edited lines. It is worth noting that *Ampelomyces* represent a natural biocontrol agent of PM, able to parasitize the mycelium and chasmothecia in turn limiting PM spread. Its reduced abundance in *MLO6/7* lines can be due to the lower colonization of PM (its natural hosts). On the other hand, the unaffected relative abundance in *NPR3* lines suggests that, even though *NPR3*-edited lines showed improved defense responses, such adjustments are not influencing the *Ampelomyces* activity. Finally, a much wider effect on the immune system of *NPR3*-edited lines can be envisaged by the improved resilience against DM and by an exclusive reduction of *Dactylonectria*, *Ilyonectria*, and *Pleosporales incertae sedis* genera, all hosting well-known grape pathogens (Probst et al., 2019), only in *NPR3*-edited plants.

Interestingly, *NPR3*-edited plants exhibited an enhanced regeneration efficiency, suggesting an indirect effect on the embryogenesis process. Indeed, if compared to *MLO*-edited plants we were able to recover a higher number of embryos even if the starting material was the same (same embryogenic calli stock and same starting quantity). Such a result was quite unexpected since, as previously reported (Dal Santo et al., 2022), the elicitation of stress responses and secondary metabolism was associated with a reduced embryogenic potential in grapevine. This unforeseen finding is quite interesting, as recalcitrance to regenerate is one of the main bottlenecks impairing the wide application of gene editing in many plant species (Atkins & Voytas, 2020). A more in-depth evaluation of the effects of *NPR3-like* editing during the regeneration phase is needed in order to uncover the molecular and biochemical signals controlling the observed enhancement of embryo regeneration.

Finally, to improve the understanding of the complex responses occurring in the edited lines, leaf samples were subjected to molecular and biochemical analyses. In particular, both *NPR3* and *MLO*-edited lines accumulated higher levels of stilbenes and polyphenols. Specifically, MLO6/7 mutants displayed a significant overaccumulation of polymerized stilbenes (viniferins). This observation can be explained by the fact that the overproduction of secondary metabolites can lead to polymerization within specific cellular environments. Although the exact mechanism remains unclear, the polymerization is a well-known process occurring for catechins (yielding proanthocyanidins and tannins) (Mannino et al., 2021) and resveratrol (yielding viniferins) (Fuloria et al., 2022). These obtained molecules possess improved stability and bioavailability compared to their monomeric equivalents, potentially enhancing their efficacy in preventing and ameliorating various pathological conditions (Langcake, 1981). In our experimental conditions, we observed a substantial reduction in total peroxide content for both mutant types, coupled with a concurrent increase in total polyphenol content. The elevation in total polyphenol contents closely correlates with the increased levels of phytoalexins. In *NPR3*-edited lines the increase in polyphenols also correlates with the strong overexpression (FC >2) of three polyphenol oxidase-encoding genes (VIT_00s0480g00060, VIT_00s0480g00070, VIT_10s0116g00560). Additionally, phenolic compounds are renowned for their antioxidant properties, and along with other secondary metabolites could have contributed to maintain the cellular redox

balance in edited grapevine plants by efficiently mitigating free radicals (Amarowicz et al., 2008). The derivatives of *t*-resveratrol, such as piceid and viniferins, also hold robust antioxidant capabilities. In fact, if the greater stability and aqueous solubility of the piceid compared to *t*-resveratrol allows a greater bioavailability, viniferins show an even greater reductive capacity due to their polymeric architecture enhancing their ability to sequester oxidizing agents (Delmas et al., 2011). Moreover, both resveratrol and its derivatives augment the activity of endogenous antioxidant enzymes within cells, including superoxide dismutase (SOD) and catalase (CAT), thereby further fortifying cells' resilience against oxidative stressors. SOD and CAT work synergistically neutralizing free radicals and peroxides, thereby mitigating oxidative damage to cells and safeguarding their structural integrity (Gülçin, 2010). In edited lines, in particular in *NPR3* ones, we observed an overexpression of catalase genes and several *Glutathione S-Transferase* (*GST*) genes (Tables S4 and S5) encoding a large protein family that catalyzes the conjugation of reduced glutathione (GSH) to various substrates preventing the oxidative stress (Neuefeind et al., 1997). For example, *GST* expression was higher in asymptomatic leaves of grapevine canes infected by esca disease (Valtaud et al., 2009). Resveratrol and its derivatives possess the ability to modulate the activity of SOD and CAT through various mechanisms. Firstly, as previously discussed, these compounds can act as direct antioxidants, effectively neutralizing free radicals and reducing peroxide generation. Furthermore, resveratrol and its derivatives can directly shield SOD and CAT from inactivation induced by oxidative agents (Gülçin, 2010). The observed reduction in total peroxide content in our experimental conditions could likely be ascribed experimentally to the combined action of both enzymatic activity and polyphenol content (Tang et al., 2010). Finally, the accumulation of stilbenes and higher activity of the antioxidant enzymes, both having a cytoprotective outcome, could also explain the reason for more stable F_v/F_m values, potentially mitigating the pleiotropic effects of *MLOs* knock-out mutants (as depicted by SPAD and F_v/F_m values) as reported in other species (Consonni et al., 2010).

CONCLUSIONS

The recent legislative proposal adopted by the European Parliament (https://www.europarl.europa.eu/doceo/document/TA-9-2024-0067_EN.html) reflects a consensus among scientific institutions, industry, and farmers on the need to exploit biotechnological approaches to start a new green revolution in agriculture (Sheridan, 2024). Indeed, gene editing represents a novel chance to exploit the potential of plant biotechnology in Europe, allowing the amelioration of cultivated plants in terms of nutritional profile, resistance to stress, and yield (Zhan et al., 2021). The present work, exploiting a Cre-lox recombinase approach, demonstrated the huge potential of biotechnology to improve viticulture sustainability producing a transgene-free edited grape plant. Indeed, by targeting two different sets of genes, we obtained immune plants as well as plants showing an improved tolerance to both *E. necator* and *P. viticola* (Figure 6). Metabolic analyses revealed a possible correlation with the accumulation of phenolic compounds, including diverse stilbenes, in both *MLO6/7* and *NPR3-like* mutants. Such an improvement not only positively influenced resilience against PM and DM, but also potentially mitigated the pleiotropic effects of *MLO6-7* defective plants already reported in other species. These results suggest that the application of NPBTs for the obtainment of improved genotypes with high level of these strong fungitoxic compounds could help to improve biotic stress resilience. Finally, we uncovered an intriguing side effect of *NPR3-like* defective calli, which displayed an improved ability to regenerate embryos when compared to *MLO*-edited calli. Additional studies are warranted to elucidate the underlying mechanisms contributing to such an effect.

EXPERIMENTAL PROCEDURES

Embryogenic calli

From late April to the beginning of May depending on the phenological stage, flower clusters of *V. vinifera* cv. Chardonnay were harvested from a vineyard located in Rauscedo (PN) and managed by Vivai Cooperativi Rauscedo (VCR). Only the basal half of the inflorescence was retained during collection. The right developmental stage of pollen was assessed following established methodologies (Gambino et al., 2007; Gribaudo et al., 2004). Subsequently, the collected flowers underwent a sterilization process involving a 15-min treatment with a sodium hypochlorite solution (1.5% available chlorine) containing 100 μL L^{-1} of Tween 20, followed by multiple rinses with sterile distilled water. Ovaries and anthers, including their filaments, were excised and cultured on PIV starter calli induction medium [Nitsch and Nitsch basal salt, Murashige and Skooge vitamins, 6% sucrose, 0.3% Gelrite, 4.5 μM 2,4-Dichlorophenoxyacetic acid (2,4 D), and 8.9 μM 6-Benzylaminopurine (BAP), pH of 5.8] (Dhekney et al., 2019; Franks et al., 1998; Gambino et al., 2007, 2021). Three months after callus induction, embryogenic calli were visually identified and transferred onto C1 proliferation medium (Nitsch and Nitsch basal salt, Murashige and Skooge vitamins, 6% sucrose, 0.5% Gelrite, 5 μM 2,4 D, and 1 μM BAP, pH of 5.8) and transferred monthly onto fresh medium (Gribaudo et al., 2004).

Vector construction

Guide RNAs (gRNAs) targeting the *VvMLO7*, *VvMLO6*, and *VvNPR3* genes (Vitvi13g00578, Vitvi13g04070, and Vitvi10g01335) (Shi et al., 2023) were evaluated using the online tool CRISPR-P (http://crispr.hzau.edu.cn/CRISPR2/) (Lei et al., 2014). The gRNAs (Table S6) were selected based on their on-target efficiency with a single gRNA designed for each gene. Additionally, an off-target analysis was performed using CRISPOR (Concordet & Haeussler, 2018) and Cas-OFFinder to ensure specificity and minimize

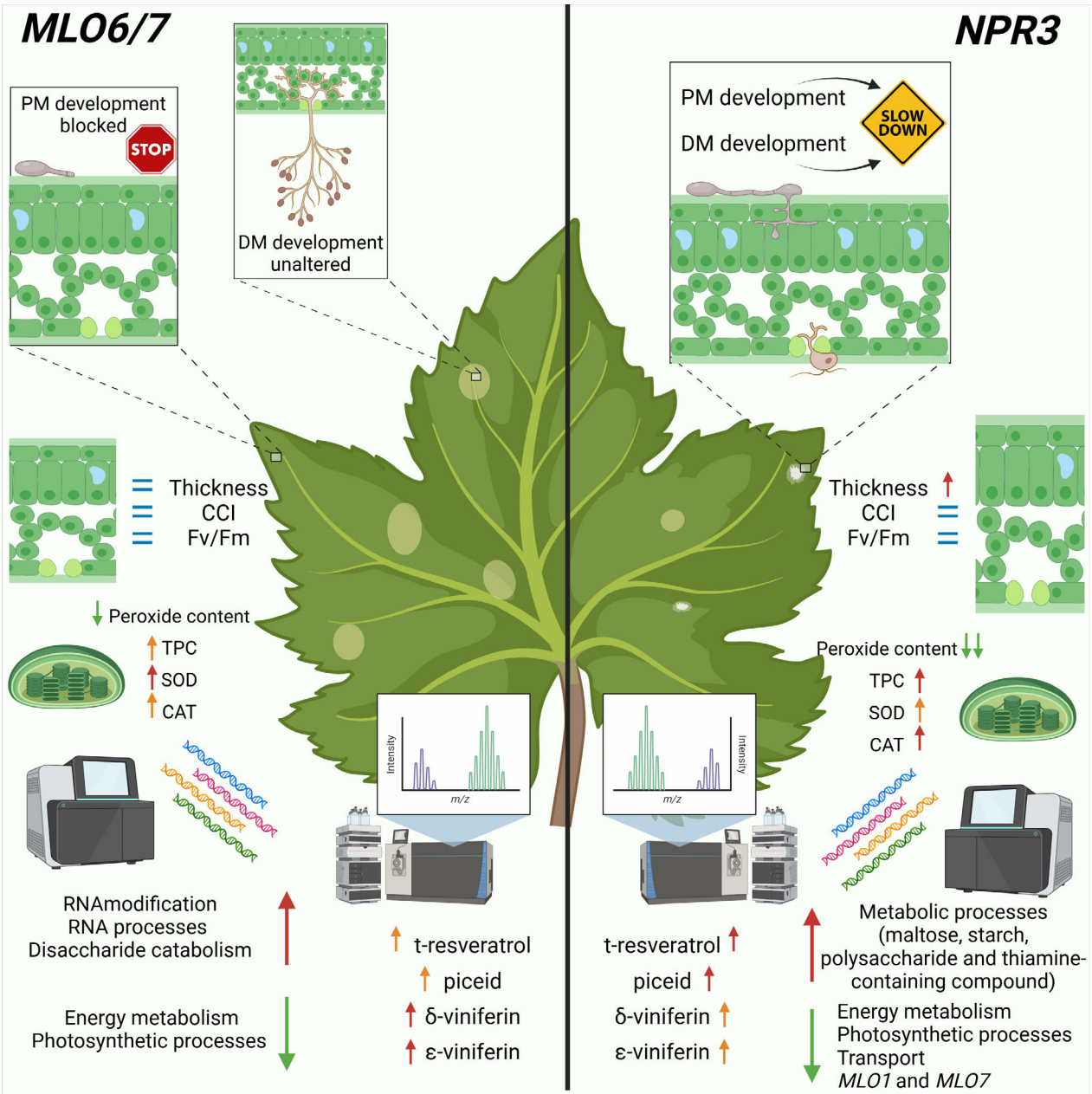

Figure 6. Overview of the main findings.
Summary of the susceptibility degree to powdery mildew (PM) and of the molecular, physiological and biochemical adjustments observed in *MLO6/7* edited (left side) and *NPR3* edited (right side) plants. Metabarcoding analysis revealed that, while in *MLO6/7* plants PM development was almost impaired, in *NPR3* plants PM development significantly lower than in wild-type plants (WT) but not that much as in *MLO6/7*. Additionally, while in *MLO6/7* plants no influence was observed on the relative abundance of other pathogens, in *NPR3* ones a significant reduction was observed. From the physiological point of view, leaf thickness, chlorophyll content index and photosystem II efficiency (F_v/F_m) were evaluated, highlighting a thicker leaf in *NPR3* plants. From the molecular point of view, similarity between *MLO6/7* and *NPR3*-edited plants were observed. From the biochemical point of view we observed an enhancement of stilbenes in both type of plants but involving different type of molecules. In *MLO6/7* plants increase in δ- and ε-viniferin was observed while piceid and resveratrol increased more in *NPR3* plants. Finally, the oxidative status was monitored revealing an increase of scavenging potential in both type of plants but with a larger extent in *NPR3* plants.

potential off-target effects (Bae et al., 2014). Used guides are listed in Table S6.

Phylogenetic placement of VvMLO6, VvMLO7, and NPR3 was calculated as previously described (Brambilla et al., 2023; Nerva et al., 2022). Briefly, sequences of *MLO* and *NPR* genes were retrieved from repositories (TAIR for *Arabidopsis*, SolGenomics for tomato, NCBI for others) and aligned using Muscle (Edgar, 2004). For MLO, 143 sequences were used and for NPR 20 sequences were used (including the *VvACT* as outgroup for both analyses). Alignments in fasta format are made available as

Data S1 (MLO) and Data S2 (NPR). Phylogenetic relationship was then calculated using the IQ-TREE webserver (Trifinopoulos et al., 2016) and then visualized in MEGA (Kumar et al., 2016). The pDIRECT_22c vector (Čermák et al., 2017) was customized, and a recombinase system based on the Cre-lox system combined to the heat-shock inducible promoter (Chong-Pérez et al., 2012; Gilbertson, 2003) was integrated (Figure S8 and sequence reported in Data S3). The vector assembly involved the insertion of a gRNA targeting each gene. In detail, for MLO knock-out, one gRNA targeting *VvMLO6* and one targeting *VvMLO7* were co-integrated, otherwise a gRNA was inserted to achieve *VvNPR3* knock-out. PCR products of gRNAs obtained following the procedure described by Čermák et al. (2017) were cloned into the previously constructed plasmid following the protocols by Lampropoulos et al. (2013). Competent cells of *Agrobacterium tumefaciens* strain GV3101 were used to transform embryogenic calli as previously described by Dhekney et al. (2008).

A. tumefaciens was initially cultured on LB agar and subsequently sub-cultured in MG/L medium to reach a final optical density (OD_{600}) of 0.8, according to Amarowicz et al. (2008) and Li et al. (2008), with only minor modifications: after MG/L culture, the cell suspension was centrifuged, resuspended in LCM medium supplemented with 100 μM acetosyringone and incubated at 28°C and 210 rpm for 3 h.

Embryogenic calli, previously conditioned according to Gribaudo et al. (2004), were co-cultured with *A. tumefaciens* (Torregrosa et al., 2015) using 600 mg L^{-1} of cefotaxime as selective agent in LCM medium to rinse embryogenic calli. Subsequently, the embryogenic calli were dried on sterile filter paper, transferred onto GS1CA medium [Nitsch and Nitsch basal salt, Murashige and Skooge vitamins, 6% sucrose, 1% Agar, 4.5 μM 2,4 D, 1 μM BAP, 10 μM 2-Napthoxyacetic acid (NOA); 20 μM Indole-3-acetic acid (IAA) pH of 5.8] (Franks et al., 1998; Gambino et al., 2007) supplemented with 450 mg L^{-1} cefotaxime, and maintained at 26°C for 9 days. Calli were sub-cultured monthly on GS1CA media supplemented with 450 mg L^{-1} cefotaxime and 100 mg L^{-1} kanamycin for 4 months. Thereafter, calli were transferred monthly onto GS1CA medium supplied with 100 mg L^{-1} kanamycin.

Embryos at the torpedo stage were transferred onto MS-SH medium (Murashige and Skooge basal salt, Murashige and Skooge vitamins, 1.5% sucrose, 0.4% Gelrite, and 10 μM BAP, pH of 5.6). After 2 months, embryos were transferred onto half-strength MS basal salts at 26°C, 200 μmol m^{-2} sec^{-1} (PPFD), and a 16/8-h day/night photoperiod. When 5 leaves were fully expanded, each node was transferred onto half-strength MS basal salts supplemented with 4 μM BAP for 1 month. Subsequently, the nodal explants were moved to MS supplemented with 2.5 μM NAA and 2.5 μM IBA for 20 days to induce root formation. The resulting explants were transferred to half-strength MS basal salts for 1 month and then to sterilized peat pellet. Among all regenerated plants, three lines for the double mutants *MLO6/MLO7* and three for the *NPR3-like* were retained for further experiments. In total 25 plants for each selected line, including wild-type embryogenic-derived plants (WT), were acclimatized in a greenhouse at the beginning of June 2023.

Editing efficiency analysis

Genomic DNA was extracted from a single leaf of each plant using the Genomic DNA Isolation Kit NORGEN (Norgen Biotech Corp). The DNA concentration was determined using a NanoDrop One Spectrophotometer (Thermo Fisher Scientific) and subsequently diluted to a final concentration of 10 ng μL^{-1}. The diluted DNA samples were used for PCR reactions using DreamTaq Green DNA polymerase (Thermo Fisher Scientific) using specific primers for Cas9 (Table S7). The initial editing efficiency was assessed through Sanger sequencing (BioFab Research srl, Italy) of the genomic regions targeted by gRNAs (Table S7). The sequencing data were analyzed using TIDE (https://tide.nki.nl/) software (Brinkman et al., 2014).

The *VvMLO7*, *VvMLO6*, and *VvNPR3* target regions of the greenhouse-acclimatized plants were screened by high-throughput sequencing. The target regions were amplified using primers and overhang Illumina adapters to generate Illumina library amplicons (Table S7). Subsequently, the library was sequenced by the Illumina NovaSeq 6000 platform at the IGA (Udine, Italy). Approximately 100 000 reads per sample were produced. Raw paired-end reads were analyzed using the CRISPResso pipeline (https://crispresso2.pinellolab.org/) and removing reads with low quality (Clement et al., 2019).

Susceptibility assay and leaf ecophysiology

After 3 months in the greenhouse, plants were attacked by a naturally occurring PM infection. When all control plants had at least three leaves with clear powdery mildew symptoms, the disease indices (incidence and severity) were collected using the Grape Assess Mobile App (University of Adelaide). For each line, four independent biological groups of observation were considered. Each biological group was made up by at least 50 observations. Five non-infected leaves for each plant were collected, lyophilized, and stored at −80°C for further analyses.

Besides PM evaluation, a controlled infection using downy mildew was performed. Ten leaves from each regenerated line were randomly collected during July. Leaves were surface washed using water and paper towel and then laid on Petri dishes containing sterile water-agar (1%). The inoculum of *P. viticola* was prepared collecting sporangia from infected leaves and then diluting to 5×10^5 sporangia/mL. After inoculation (1 mL per leaf) leaves were incubated at 24°C with a 16–8 light–dark cycle. Development of leaf symptoms (i.e., emergence of sporangia from the leaves) were checked 7 days after inoculation. Descriptor 452-1 of the International Organization of Vine and Wine (OIV) were used to determine leaf resistance to downy mildew. Briefly, each leaf was visually checked and assigned to a class among the following: class 1—61 to 100% of surface covered with sporulation, class 2—41 to 60% of surface covered with sporulation, class 3—21 to 40% of surface covered with sporulation, class 4—1 to 20% of surface covered with sporulation, class 5—0% of surface covered with sporulation. Control leaves ($n = 3$) were kept without inoculation to exclude previous infections naturally occurring in the greenhouse. The experiment was repeated twice with a 15-day delay between the two trials, in order to confirm the results.

Measurements to determine chlorophyll fluorescence parameters (F_v/F_m), relative chlorophyll content (CCI), and leaf thickness were carried out using a MultispeQ v2.0 device controlled by PhotosynQ software (Kuhlgert et al., 2016). Records were taken on ten fully formed non-senescing leaves for each line, selecting one leaf per plant growing between the 4th and 6th shoot from the top.

Nucleic acid extraction, sequencing, and bioinformatics

For molecular assays, three independent biological replicates were obtained for each condition by pooling five asymptomatic leaves randomly selected every five vines of the 25 acclimatized plants (1 leaf × 5 plants × 3 biological replicates: each set of five plants therefore represented an independent biological replicate). Attention was paid to randomly collect asymptomatic leaves also

from untreated plants. This approach was adopted with the aim of investigating the specific defense responses established in the edited vines regardless of the occurrence of visible symptoms.

Genomic DNA and total RNA were isolated from lyophilized leaves using Genomic DNA Isolation Kit NORGEN (Norgen Biotech Corp) and Spectrum plant total RNA kit (Sigma-Aldrich, St. Louis, MO, USA), respectively, according to the manufacturer's instructions.

DNA and RNA concentrations were evaluated using a NanoDrop one Spectrophotometer (Thermo Fisher Scientific, Waltham, MA, USA) and integrity was confirmed on agarose gel. To proceed with RNA-seq analysis, at least 2 μg for each sample was sent to Macrogen Inc. (Europe) for cDNA library construction and sequencing using NovaSeq. Furthermore, Illumina tag screening of the ITS2 region of the rDNA was performed by Macrogen Inc. (South Korea) using primers ITS3-ITS4 on a MiSeq Illumina apparatus. Trimmed sequences were analyzed with DADA2 and sequence variants were taxonomically classified using the UNITE database, as previously described (Nerva et al., 2021). Analysis of transcripts was performed using the Artificial Intelligence RNA-seq Software AIR (accessible at https://transcriptomics.cloud). Transcripts were annotated using the V1 annotation of the grapevine genome (Grimplet et al., 2012); functional classification, GO enrichment analysis, and identification of differentially expressed genes (DEGs) were performed as previously described (Nerva et al., 2022).

Heat shock treatments and evaluation of copy number variation through qPCR

Three-week-old grapevine plants acclimatized in the greenhouse and displaying knock-out of target genes were incubated in a temperature-controlled chamber at 45°C for 24 h for three cycles with a 48-h interval between treatments. To assess the CNV resulting from heat treatments, a single leaf (developed after the heat treatment) from each plant was collected, lyophilized, and the genomic DNA was extracted and used for qPCR analysis using a custom-made calibration curve (Dalla Costa et al., 2009; Lee et al., 2006). Quantification of the *NPTII* copy number was employed to quantify T-DNA insertions (Table 1).

Calibration curves were constructed by amplifying the *VvCHI* fragment from Chardonnay leaf using primers listed in Table S7. Briefly, PCR product was cloned into pGEM-T Easy vector, which already contained a fragment of the *NPTII* gene cloned from pDIRECT_22c. The final plasmid pGEM:CHI:NPTII was purified and quantified using NanoDrop One Spectrophotometer and its molarity was calculated using the NEBioCalculator online tool (version 1.15.5). A 10-fold serial dilution series of the pGEM:CHI:NPTII plasmid was used to construct the calibration curve according to Dalla Costa et al. (2009).

Each amplification was followed by melting curve analysis (60–94°C) with a heating rate of 0.5°C every 15 sec. All reactions were performed in duplicate with nuclease-free water as negative control. Estimation of the *NPTII* insertion copies in transgenic grapevines was calculated using the following formula: (*NPTII* gene copy number/*VvCHI* copy number) × 2.

Biochemical analyses

About 100 mg of lyophilized leaves (the same used for RNA-seq analysis) were used for the biochemical analyses. Briefly, extraction was performed using 1 mL of a 1:1 (*v/v*) mixture of Methyl-t-Butyl Ether (MTBE) and Methanol (MetOH), as previously described (Liu et al., 2013). Following vortex mixing, the samples were sonicated for 15 min at 4°C. Subsequently, 0.5 mL of 0.1% (*v/v*) HCl was added. After a 5-min incubation at 4°C, the samples were centrifuged at 10 000*g* for 10 min at 4°C. The upper MTBE phase was transferred, dried under nitrogen flow at constant flow, and resuspended in 100 μL of 50% (*v/v*) propanol. Accordingly, samples were injected into a HPLC-DAD-ESI-MS/MS apparatus, and the analytical separation of phytoalexins was conducted employing a binary solvent system consisting of water acidified with 0.1% (*v/v*) formic acid (solvent A) and methanol acidified to 0.1% (*v/v*) with formic acid (solvent B). A Kinetecs C18 column (130 Å, 1.7 μm, 2.1 × 100 mm) was utilized for the separation. The gradient profile was as follows: 0–8 min with 95% (*v/v*) A, 8–12 min decreasing A to 75% (*v/v*), 12–16 min decreasing A to 55% (*v/v*), 16–32 min decreasing A to 25% (*v/v*), and subsequently reduced to 5% (*v/v*) at 45 min. Solvent A concentration was maintained for 10 min. Throughout the chromatographic run, the flow rate was set at 0.2 mL min^{-1}, with a 10 μL injection volume. Chromatographic conditions were restored to initial conditions and maintained for 8 min before the next injection (Sun et al., 2006). Phytoalexins were quantified using different concentrations of *t*-resveratrol, δ-viniferin, and ε-viniferin by plotting peak areas against concentrations, and linear regression was applied for curve fitting. Original standards of *t*-resveratrol (purity ≥99%), piceid (purity ≥99%), and viniferins (purity ≥95%) purchased from Merck KGaA were used to prepare the calibration curves. Limits of detection (LOD) and limits of quantification (LOQ) were calculated for each standard following the method described by Cao et al. (2020).

Total phenolic content (TPC) was quantified preparing the ethanolic extracts of the lyophilized leaves and assessed using the Folin–Ciocalteu method, which entails the reduction of phosphotungstic-phosphomolybdic acid to blue pigments in an alkaline medium. This method follows the procedure outlined by Folin and Denis, as previously described by Singleton (1966). For quantification, a calibration curve with gallic acid (GA) was used, and the results were expressed as milligrams of GA equivalents (GAE) per 100 g of fresh weight (FW). Each sample was measured in triplicate to ensure accuracy and reliability of the data. This approach allows for a precise evaluation of the phenolic content, which is crucial for understanding the antioxidant properties of the extracts.

The total peroxide content was measured using a Peroxide Assay Kit from Abnova (St. Louis, MO, USA). To begin, 50 mg of lyophilized leaves were ground in liquid nitrogen and extracted with milli-Q water at a ratio of 1:10 (w/v). Following extraction, the samples were centrifuged at 15 000×*g* for 10 min, and the resulting supernatant was used for the assay. For the assay, 200 μL of detection reagent was added to each 40 μL sample in a flat-bottom 96-well plate. After a 30-min incubation period, the absorbance was measured at 600 nm using a microplate reader. The H_2O_2 content was determined by comparing the absorbance values to a standard curve generated from serial dilutions of a 3% H_2O_2 standard.

Lyophilized leaves were pulverized and homogenized with a mortar and pestle to determine enzyme activities. The ground material was then extracted in a solution containing 62.5 mM Tris–HCl (pH 7), 10% (v/v) glycerol, 2% (w/v) Sodium Dodecyl Sulfate (SDS), 1 mM EDTA, and 1 mM phenylmethylsulfonyl fluoride (PMSF). The mixture was centrifuged at 5000*g* for 10 min at 4°C, and the supernatant was collected for subsequent enzymatic assays. The total protein concentration was measured using the Lowry method to normalize the enzymatic activities (Assink Junior et al., 2023). Enzymatic activities for Superoxide Dismutase (SOD; ab65354) and Catalase (CAT; ab83464) were determined using

commercial kits from Abcam, following the manufacturer's instructions and according to Agliassa et al. (2021).

Statistical analysis

For the PM disease indices, biochemical data, and MultispeQ data, analysis of variance (ANOVA) was conducted using the SPSS software package (v. 23, SPSS Inc). For DM disease resistance analysis chi-squared test was calculated. The Tukey's HSD post hoc test was used when ANOVA showed significant differences at a probability level of $P \leq 0.05$. The standard deviation (SD) of all means was calculated.

ACCESSION NUMBERS

The GenBank accession numbers of the sequences reported in this paper are:

- RNA-seq study: BioProject PRJNA1120233, BioSample SAMN 41684953 to SAMN41684955, SRA SRR29288783 to SRR292 88785.
- ITS metabarcoding: BioProject PRJNA1119720, BioSample SAMN41663148 to SAMN41663150, SRA SRR29272512 to SRR 29272514.
- NGS amplicon on-target genomic sequences: BioProject PRJNA1119700, BioSample SAMN41662708 to SAMN41662739, SRA SRR29272386 to SRR29272402.

All the other study data are included in the article and supporting information.

AUTHOR CONTRIBUTIONS

LN and WC conceived and supported this study; LN, WC and LM designed the experiments; LM performed research with assistance from GM, IB, GG, IP, CP, CMB, AS, EZ, RV, WC and LN; LM, GM, GG, WC and LN analyzed the data; LM, GM, IB, WC and LN wrote the manuscript; and all authors reviewed and edited the manuscript.

ACKNOWLEDGMENTS

Part of the work was conducted within the Shield4Grape project (Grant number 101135088) funded by the European Commission in the framework of the Horizon Europe program and within the BIOTECH-VITECH project funded by the Italian Ministry of Agriculture, Food Sovereignty and Forestry. Views and opinions expressed are, however, those of the authors only. Neither the European Union nor the granting authority nor the European Commission can be held responsible for them. The authors thank Alison Garside for the manuscript English editing service. Figure 6 has been created in BioRender (https://biorender.com/z80s157).

CONFLICT OF INTEREST

The authors declare that they have no conflict of interests. This article does not contain any studies with human or animal participants.

DATA AVAILABILITY STATEMENT

The data that support the findings of this study are openly available. The GenBank accession numbers of the sequences reported in this paper are indicated in the *Accession numbers* section. All the other study data are included in the article and supporting information.

SUPPORTING INFORMATION

Additional Supporting Information may be found in the online version of this article.

Data S1. Alignments of MLO proteins. Sequences of 141 MLO proteins, including protein sequences from grapevine were aligned using Muscle.

Data S2. Alignments of NPR proteins. Sequences of 19 NPR proteins, including protein sequences from grapevine were aligned using Muscle.

Data S3. Vector sequence. The modified sequence of the pDIR-ECT_22C vector including Cre/loxP cassette and sites.

Figure S1. Phylogenetic placement of *Vv*MLO proteins. The phylogenetic placement of *Vitis vinifera* (*Vv*) MLO proteins has been inferred using the IQ-TREE webserver. Sequences from *Malus domestica* (*Md*), *Glycine max* (*Gm*), *Prunus persica* (*Pp*), *Solanum lycopersicum* (*Sl*), *Fragaria vesca* (*Fv*), and *Arabidopsis thaliana* (*At*) have been used. The red arrow indicates the clade hosting MLO6 and MLO7, the two targets of the present work.

Figure S2. Phylogenetic placement of *Vv*NPR proteins. The phylogenetic placement of *Vitis vinifera* (*Vv*) NPR proteins has been inferred using the IQ-TREE webserver. The red arrow indicates the clade hosting the target (NPR3) of the present work.

Figure S3. Picture of representative plants. Plants acclimatized from the *in vitro* condition did not show phenotypic differences when compared to WT plants. From left to right, one representative plant for each line (*NPR3*#4, #9, and #15, *MLO6-7*#1, #3, #9, and WT) has been chosen.

Figure S4. Gel electrophoresis of the Cre and Cas PCR products. PCR products from the negative MLO6-7#3 plant were run in a 1% agarose gel together with positive and negative controls. (A) is the PCR product from the *NCED3* gene, representing a positive control for the plant DNA. (B)–(D) are the amplicon from PCR at 35, 40, and 45 cycles, respectively. In each panel, from left to right: MM, molecular marker (1 kb plus, the first thicker band represents the 500 bp, the second thicker band represents the 1000 bp); (1) plant harboring T-DNA with a copy number of 1; (2) MLO6-7#3 T-DNA-free plant; (3) MLO6-7#3 plant with a copy number of 0.3; (4) WT plant (negative control); (5) MLO6-7#3 plant with a copy number of 0.1.

Figure S5. Upregulated metabolic pathways as identified through RNA-seq analysis. Upregulated genes in *MLO6-7* edited versus WT lines (A-B-C), *NPR3-like* edited versus WT (D-E-F) and *MLO6-7* edited versus *NPR3-like* edited were analyzed to identify genes belonging to specific metabolic routes. (A, D, G) Pathways showing an enrichment of terms in the dataset. Darker colors (from yellow to orange) refer to a more represented pathway. (B, E, H) percentages of gene ontology (GO) terms belonging to each specific group. (C, F, I) percentages of genes belonging to specific terms or functions.

Figure S6. Redox-active balance measured through UV/Vis determination. (A) displays the total peroxide content expressed as mmol H_2O_2 g^{-1} of dry (DW) material ($n = 3$), while (B) shows the total phenolic compound content expressed as mg of gallic acid equivalent (GAE) g^{-1} of dry weight material ($n = 3$). Enzymatic activities of superoxide dismutase (SOD) and catalase (CAT) are depicted in (C) and (D), respectively, measured as enzymatic activity (U) relative to the total protein content determined as described in the materials and methods section ($n = 3$ each). Lowercase letters above bars indicate significant differences among the samples, as determined by ANOVA followed by Tukey's post-

hoc test. All data in bar charts represent mean values ± standard deviation bars.

Figure S7. Map of plasmid developed in the present study. The main sequences of the vector have been annotated, including the HSP promoter, the Cre encoding sequence, and the loxP sites.

Figure S8. Map of the modified pDIRECT_22C vector.

Table S1. Differential abundances of taxa across edited lines. Average abundances (Mean), standard deviation (SD), and significance in comparison with WT plants (*P*-value) of each edited line were calculated using the ANCOM-BC functions.

Table S2. Differential abundances of taxa across edited targets. Average abundances (Mean), standard deviation (SD), and significance in comparison with WT plants (*P*-value) were calculated using the ANCOM-BC functions.

Table S3. List of differentially expressed genes in *MLO6-7* edited lines. Differentially regulated genes with a fold-change (FC) higher than 1 are reported considering the comparison between *MLO6-7* edited lines and WT plants.

Table S4. List of differentially expressed genes in *NPR3-like* edited lines. Differentially regulated genes with a fold-change (FC) higher than 1 are reported considering the comparison between *NPR3-like* edited lines and WT plants.

Table S5. List of differentially expressed genes in *MLO6-7* versus *NPR3-like* edited lines. Differentially regulated genes with a fold-change (FC) higher than 1 are reported considering the comparison between *MLO6-7* versus *NPR3-like* edited lines.

Table S6. Selected gRNAs. List of the gRNAs used in this study. For each gRNA, the PAM site is underlined.

Table S7. Oligonucleotides. List of the oligonucleotides used in this study.

REFERENCES

Acevedo-Garcia, J., **Kusch, S.** & **Panstruga, R.** (2014) Magical mystery tour: MLO proteins in plant immunity and beyond. *New Phytologist*, **204**, 273–281.

Agliassa, C., **Mannino, G.**, **Molino, D.**, **Cavalletto, S.**, **Contartese, V.**, **Bertea, C.M.** ***et al.*** (2021) A new protein hydrolysate-based biostimulant applied by fertigation promotes relief from drought stress in *Capsicum annuum* L. *Plant Physiology and Biochemistry*, **166**, 1076–1086.

Amarowicz, R., **Narolewska, O.**, **Karamac, M.**, **Kosinska, A.** & **Weidner, S.** (2008) Grapevine leaves as a source of natural antioxidants. *Polish Journal of Food and Nutrition Sciences*, **58**, 73–78.

Anderson, R., **Bayer, P.E.** & **Edwards, D.** (2020) Climate change and the need for agricultural adaptation. *Current Opinion in Plant Biology*, **56**, 197–202.

Assink Junior, E.J., **Jesus, P.C.d.** & **Borges, E.M.** (2023) Whey protein analysis using the Lowry assay and 96-well-plate digital images acquired using smartphones. *Journal of Chemical Education*, **100**, 2329–2338.

Atkins, P.A. & **Voytas, D.F.** (2020) Overcoming bottlenecks in plant gene editing. *Current Opinion in Plant Biology*, **54**, 79–84.

Bae, S., **Park, J.** & **Kim, J.-S.** (2014) Cas-OFFinder: a fast and versatile algorithm that searches for potential off-target sites of Cas9 RNA-guided endonucleases. *Bioinformatics*, **30**, 1473–1475.

Brambilla, M., **Chiari, G.**, **Commisso, M.**, **Nerva, L.**, **Musetti, R.**, **Petraglia, A.** ***et al.*** (2023) Glutamate dehydrogenase in "Liverworld"—a study in selected species to explore a key enzyme of plant primary metabolism in Marchantiophyta. *Physiologia Plantarum*, **175**, e14071.

Brinkman, E.K., **Chen, T.**, **Amendola, M.** & **van Steensel, B.** (2014) Easy quantitative assessment of genome editing by sequence trace decomposition. *Nucleic Acids Research*, **42**, e168.

Büschges, R., **Hollricher, K.**, **Panstruga, R.**, **Simons, G.**, **Wolter, M.**, **Frijters, A.** ***et al.*** (1997) The barley *Mlo* gene: a novel control element of plant pathogen resistance. *Cell*, **88**, 695–705.

Cao, D., **Barbier, F.**, **Yoneyama, K.** & **Beveridge, C.A.** (2020) A rapid method for quantifying RNA and phytohormones from a small amount of plant tissue. *Frontiers in Plant Science*, **11**, 605069. Available from: https://doi.org/10.3389/fpls.2020.605069

Ceasar, S.A. & **Ignacimuthu, S.** (2023) CRISPR/Cas genome editing in plants: Dawn of *Agrobacterium* transformation for recalcitrant and transgene-free plants for future crop breeding. *Plant Physiology and Biochemistry*, **196**, 724–730.

Čermák, T., **Curtin, S.J.**, **Gil-Humanes, J.**, **Čegan, R.**, **Kono, T.J.Y.**, **Konečná, E.** ***et al.*** (2017) A multipurpose toolkit to enable advanced genome engineering in plants. *The Plant Cell*, **29**, 1196–1217.

Chang, M., **Zhao, J.**, **Chen, H.**, **Li, G.**, **Chen, J.**, **Li, M.** ***et al.*** (2019) PBS3 protects EDS1 from proteasome-mediated degradation in plant immunity. *Molecular Plant*, **12**, 678–688.

Chong-Pérez, B., **Kosky, R.G.**, **Reyes, M.**, **Rojas, L.**, **Ocaña, B.**, **Tejeda, M.** ***et al.*** (2012) Heat shock induced excision of selectable marker genes in transgenic banana by the Cre-lox site-specific recombination system. *Journal of Biotechnology*, **159**, 265–273.

Clemens, M., **Faralli, M.**, **Lagreze, J.**, **Bontempo, L.**, **Piazza, S.**, **Varotto, C.** ***et al.*** (2022) *VvEPFL9*-1 knock-out via CRISPR/Cas9 reduces stomatal density in grapevine. *Frontiers in Plant Science*, **13**, 878001.

Clement, K., **Rees, H.**, **Canver, M.C.**, **Gehrke, J.M.**, **Farouni, R.**, **Hsu, J.Y.** ***et al.*** (2019) CRISPResso2 provides accurate and rapid genome editing sequence analysis. *Nature Biotechnology*, **37**, 224–226.

Concordet, J.-P. & **Haeussler, M.** (2018) CRISPOR: intuitive guide selection for CRISPR/Cas9 genome editing experiments and screens. *Nucleic Acids Research*, **46**, W242–W245.

Consonni, C., **Bednarek, P.**, **Humphry, M.**, **Francocci, F.**, **Ferrari, S.**, **Harzen, A.** ***et al.*** (2010) Tryptophan-derived metabolites are required for antifungal defense in the Arabidopsis *mlo2* mutant. *Plant Physiology*, **152**, 1544–1561.

Consonni, C., **Humphry, M.E.**, **Hartmann, H.A.**, **Livaja, M.**, **Durner, J.**, **Westphal, L.** ***et al.*** (2006) Conserved requirement for a plant host cell protein in powdery mildew pathogenesis. *Nature Genetics*, **38**, 716–720.

Dal Santo, S., **de Paoli, E.**, **Pagliarani, C.**, **Amato, A.**, **Celii, M.**, **Boccacci, P.** ***et al.*** (2022) Stress responses and epigenomic instability mark the loss of somatic embryogenesis competence in grapevine. *Plant Physiology*, **188**, 490–508.

Dalla Costa, L., **Piazza, S.**, **Campa, M.**, **Flachowsky, H.**, **Hanke, M.-V.** & **Malnoy, M.** (2016) Efficient heat-shock removal of the selectable marker gene in genetically modified grapevine. *Plant Cell, Tissue and Organ Culture (PCTOC)*, **124**, 471–481.

Dalla Costa, L., **Piazza, S.**, **Pompili, V.**, **Salvagnin, U.**, **Cestaro, A.**, **Moffa, L.** ***et al.*** (2020) Strategies to produce T-DNA free CRISPRed fruit trees via *Agrobacterium tumefaciens* stable gene transfer. *Scientific Reports*, **10**, 1–14.

Dalla Costa, L., **Vaccari, I.**, **Mandolini, M.** & **Martinelli, L.** (2009) Elaboration of a reliable strategy based on real-time PCR to characterize genetically modified plantlets and to evaluate the efficiency of a marker gene removal in grape (Vitis spp.). *Journal of Agricultural and Food Chemistry*, **57**, 2668–2677.

Delmas, D., **Aires, V.**, **Limagne, E.**, **Dutartre, P.**, **Mazué, F.**, **Ghiringhelli, F.** ***et al.*** (2011) Transport, stability, and biological activity of resveratrol. *Annals of the New York Academy of Sciences*, **1215**, 48–59.

Dhekney, S., **Li, Z.**, **Dutt, M.** & **Gray, D.** (2008) *Agrobacterium*-mediated transformation of embryogenic cultures and plant regeneration in *Vitis rotundifolia* Michx.(muscadine grape). *Plant Cell Reports*, **27**, 865–872.

Dhekney, S., **Sessions, S.**, **Brungart-Rosenberg, M.**, **Claflin, C.**, **Li, Z.** & **Gray, D.** (2019) Genetic modification of grapevine embryogenic cultures. In: Walker, J.M. (Ed.) *Transgenic plants: methods and protocols*. Berlin: Springer, pp. 191–201.

Ding, Y., **Sun, T.**, **Ao, K.**, **Peng, Y.**, **Zhang, Y.**, **Li, X.** ***et al.*** (2018) Opposite roles of salicylic acid receptors NPR1 and NPR3/NPR4 in transcriptional regulation of plant immunity. *Cell*, **173**, 1454–1467.

Dutt, M., **Barthe, G.**, **Irey, M.** & **Grosser, J.** (2015) Transgenic citrus expressing an Arabidopsis *NPR1* gene exhibit enhanced resistance against Huanglongbing (HLB; Citrus Greening). *PLoS One*, **10**, e0137134.

Edgar, R.C. (2004) MUSCLE: multiple sequence alignment with high accuracy and high throughput. *Nucleic Acids Research*, **32**, 1792–1797.

Éva, C., **Téglás, F.**, **Zelenyánszki, H.**, **Tamás, C.**, **Juhász, A.**, **Mészáros, K.** ***et al.*** (2018) Cold inducible promoter driven Cre-lox system proved to be highly efficient for marker gene excision in transgenic barley. *Journal of Biotechnology*, **265**, 15–24.

Fan, Y., **Guo, F.**, **Wu, R.**, **Chen, Z.** & **Li, Z.** (2023) First report of *Colletotrichum gloeosporioides* causing anthracnose on grapevine (*Vitis vinifera*) in Shaanxi province, China. *Plant Disease*, **107**, 2249.

Feechan, A., **Jermakow, A.M.**, **Torregrosa, L.**, **Panstruga, R.** & **Dry, I.B.** (2008) Identification of grapevine *MLO* gene candidates involved in susceptibility to powdery mildew. *Functional Plant Biology*, **35**, 1255–1266.

Fernàndez-Martínez, J., **Zacchini, M.**, **Elena, G.**, **Fernández-Marín, B.** & **Fleck, I.** (2013) Effect of environmental stress factors on ecophysiological traits and susceptibility to pathogens of five Populus clones throughout the growing season. *Tree Physiology*, **33**, 618–627.

Fister, A.S., **Landherr, L.**, **Maximova, S.N.** & **Guiltinan, M.J.** (2018) Transient expression of CRISPR/Cas9 machinery targeting *TcNPR3* enhances defense response in *Theobroma cacao*. *Frontiers in Plant Science*, **9**, 329023.

Franks, T., **Gang He, D.** & **Thomas, M.** (1998) Regeneration of transgenic shape *Vitis vinifera* L. Sultana plants: genotypic and phenotypic analysis. *Molecular Breeding*, **4**, 321–333.

Freh, M., **Reinstädler, A.**, **Neumann, K.D.**, **Neumann, U.** & **Panstruga, R.** (2024) The development of pleiotropic phenotypes in powdery mildew-resistant barley and *Arabidopsis thaliana mlo* mutants is linked to nitrogen availability. *Plant, Cell & Environment*, **47**, 2360–2374.

Fu, Z.Q., **Yan, S.**, **Saleh, A.**, **Wang, W.**, **Ruble, J.**, **Oka, N.** ***et al.*** (2012) *NPR3* and *NPR4* are receptors for the immune signal salicylic acid in plants. *Nature*, **486**, 228–232.

Fuloria, S., **Sekar, M.**, **Khattulanuar, F.S.**, **Gan, S.H.**, **Rani, N.N.I.M.**, **Ravi, S.** ***et al.*** (2022) Chemistry, biosynthesis and pharmacology of viniferin: potential resveratrol-derived molecules for new drug discovery, development and therapy. *Molecules*, **27**, 5072.

Gambino, G., **Moine, A.**, **Boccacci, P.**, **Perrone, I.** & **Pagliarani, C.** (2021) Somatic embryogenesis is an effective strategy for dissecting chimerism phenomena in *Vitis vinifera* cv Nebbiolo. *Plant Cell Reports*, **40**, 205–211.

Gambino, G., **Nuzzo, F.**, **Moine, A.**, **Chitarra, W.**, **Pagliarani, C.**, **Petrelli, A.** ***et al.*** (2024) Genome editing of a recalcitrant wine grape genotype by lipofectamine-mediated delivery of CRISPR/Cas9 ribonucleoproteins to protoplasts. *The Plant Journal*, **119**, 404–412.

Gambino, G., **Ruffa, P.**, **Vallania, R.** & **Gribaudo, I.** (2007) Somatic embryogenesis from whole flowers, anthers and ovaries of grapevine (*Vitis* spp.). *Plant Cell, Tissue and Organ Culture*, **90**, 79–83.

Gao, Q., **Wang, C.**, **Xi, Y.**, **Shao, Q.**, **Li, L.** & **Luan, S.** (2022) A receptor–channel trio conducts Ca^{2+} signalling for pollen tube reception. *Nature*, **607**, 534–539.

Gilbertson, L. (2003) Cre–lox recombination: Cre-ative tools for plant biotechnology. *Trends in Biotechnology*, **21**, 550–555.

Giudice, G., **Moffa, L.**, **Varotto, S.**, **Cardone, M.F.**, **Bergamini, C.**, **De Lorenzis, G.** ***et al.*** (2021) Novel and emerging biotechnological crop protection approaches. *Plant Biotechnology Journal*, **19**, 1495–1510.

Glazebrook, J., **Rogers, E.E.** & **Ausubel, F.M.** (1996) Isolation of *Arabidopsis* mutants with enhanced disease susceptibility by direct screening. *Genetics*, **143**, 973–982.

Gómez-Muñoz, N., **Velázquez, K.**, **Vives, M.C.**, **Ruiz-Ruiz, S.**, **Pina, J.A.**, **Flores, R.** ***et al.*** (2017) The resistance of sour orange to *Citrus tristeza* virus is mediated by both the salicylic acid and RNA silencing defence pathways. *Molecular Plant Pathology*, **18**, 1253–1266.

Goyal, N., **Bhatia, G.**, **Garewal, N.**, **Upadhyay, A.** & **Singh, K.** (2021) Identification of defense related gene families and their response against powdery and downy mildew infections in *Vitis vinifera*. *BMC Genomics*, **22**, 1–16.

Gribaudo, I., **Gambino, G.**, **Boccacci, P.**, **Perrone, I.** & **Cuozzo, D.** (2017) A multi-year study on the regenerative potential of several *Vitis* genotypes. *Acta Horticulturae*, **1155**, 45–50.

Gribaudo, I., **Gambino, G.** & **Vallania, R.** (2004) Somatic embryogenesis from grapevine anthers: the optimal developmental stage for collecting explants. *American Journal of Enology and Viticulture*, **55**, 427–430.

Grimplet, J., **van Hemert, J.**, **Carbonell-Bejerano, P.**, **Díaz-Riquelme, J.**, **Dickerson, J.**, **Fennell, A.** ***et al.*** (2012) Comparative analysis of grapevine whole-genome gene predictions, functional annotation, categorization and integration of the predicted gene sequences. *BMC Research Notes*, **5**, 1–10.

Gülçin, İ. (2010) Antioxidant properties of resveratrol: a structure–activity insight. *Innovative Food Science & Emerging Technologies*, **11**, 210–218.

Hassan, S., **Nisa, M.**, **Wani, A.H.**, **Majid, M.**, **Jan, N.** & **Bhat, M.Y.** (2022) First report of Chaetomium globosum causing leaf spot disease of *Solanum melongena* in Kashmir Valley, India. *New Disease Reports*, **46**, e12119.

Humphry, M., **Reinstaedler, A.**, **Ivanov, S.**, **Bisseling, T.** & **Panstruga, R.** (2011) Durable broad-spectrum powdery mildew resistance in pea er1 plants is conferred by natural loss-of-function mutations in *PsMLO1*. *Molecular Plant Pathology*, **12**, 866–878.

Jaillon, O., **Aury, J.-M.**, **Noel, B.**, **Policriti, A.**, **Clepet, C.**, **Casagrande, A.** ***et al.*** (2007) The grapevine genome sequence suggests ancestral hexaploidization in major angiosperm phyla. *Nature*, **449**, 463–467.

Khattri, A., **Nandy, S.** & **Srivastava, V.** (2011) Heat-inducible Cre-lox system for marker excision in transgenic rice. *Journal of Biosciences*, **36**, 37–42.

Kim, K.-H., **Kabir, E.** & **Jahan, S.A.** (2017) Exposure to pesticides and the associated human health effects. *Science of the Total Environment*, **575**, 525–535.

Kim, M.C., **Panstruga, R.**, **Elliott, C.**, **Müller, J.**, **Devoto, A.**, **Yoon, H.W.** ***et al.*** (2002) Calmodulin interacts with MLO protein to regulate defence against mildew in barley. *Nature*, **416**, 447–451.

Kuhlgert, S., **Austic, G.**, **Zegarac, R.**, **Osei-Bonsu, I.**, **Hoh, D.**, **Chilvers, M.I.** ***et al.*** (2016) MultispeQ Beta: a tool for large-scale plant phenotyping connected to the open PhotosynQ network. *Royal Society Open Science*, **3**, 160592.

Kumar, S., **Stecher, G.** & **Tamura, K.** (2016) MEGA7: molecular evolutionary genetics analysis version 7.0 for bigger datasets. *Molecular Biology and Evolution*, **33**, 1870–1874.

Lampropoulos, A., **Sutikovic, Z.**, **Wenzl, C.**, **Maegele, I.**, **Lohmann, J.U.** & **Forner, J.** (2013) GreenGate-a novel, versatile, and efficient cloning system for plant transgenesis. *PLoS One*, **8**, e83043.

Langcake, P. (1981) Disease resistance of *Vitis* spp. and the production of the stress metabolites resveratrol, ε-viniferin, α-viniferin and pterostilbene. *Physiological Plant Pathology*, **18**, 213–226.

Le Henanff, G., **Heitz, T.**, **Mestre, P.**, **Mutterer, J.**, **Walter, B.** & **Chong, J.** (2009) Characterization of *Vitis vinifera NPR1* homologs involved in the regulation of pathogenesis-related gene expression. *BMC Plant Biology*, **9**, 1–14.

Lee, C., **Kim, J.**, **Shin, S.G.** & **Hwang, S.** (2006) Absolute and relative QPCR quantification of plasmid copy number in *Escherichia coli*. *Journal of Biotechnology*, **123**, 273–280.

Lei, Y., **Lu, L.**, **Liu, H.-Y.**, **Li, S.**, **Xing, F.** & **Chen, L.-L.** (2014) CRISPR-P: a web tool for synthetic single-guide RNA design of CRISPR-system in plants. *Molecular Plant*, **7**, 1494–1496.

Li, M.-Y., **Jiao, Y.-T.**, **Wang, Y.-T.**, **Zhang, N.**, **Wang, B.-B.**, **Liu, R.-Q.** ***et al.*** (2020) CRISPR/Cas9-mediated *VvPR4b* editing decreases downy mildew resistance in grapevine (*Vitis vinifera* L.). *Horticulture Research*, **7**, 149.

Li, S., **Lin, D.**, **Zhang, Y.**, **Deng, M.**, **Chen, Y.**, **Lv, B.** ***et al.*** (2022) Genome-edited powdery mildew resistance in wheat without growth penalties. *Nature*, **602**, 455–460.

Li, Z.T., **Dhekney, S.**, **Dutt, M.** & **Gray, D.** (2008) An improved protocol for *Agrobacterium*-mediated transformation of grapevine (*Vitis vinifera* L.). *Plant Cell, Tissue and Organ Culture*, **93**, 311–321.

Liu, C., **Wang, L.**, **Wang, J.**, **Wu, B.**, **Liu, W.**, **Fan, P.** ***et al.*** (2013) Resveratrols in *Vitis* berry skins and leaves: their extraction and analysis by HPLC. *Food Chemistry*, **136**, 643–649.

Liu, Y., **Sun, T.**, **Sun, Y.**, **Zhang, Y.**, **Radojičić, A.**, **Ding, Y.** ***et al.*** (2020) Diverse roles of the salicylic acid receptors NPR1 and NPR3/NPR4 in plant immunity. *Plant Cell*, **32**, 4002–4016.

Malhi, G.S., **Kaur, M.** & **Kaushik, P.** (2021) Impact of climate change on agriculture and its mitigation strategies: a review. *Sustainability*, **13**, 1318.

Mannino, G., **Chinigò, G.**, **Serio, G.**, **Genova, T.**, **Gentile, C.**, **Munaron, L.** ***et al.*** (2021) Proanthocyanidins and where to find them: a meta-analytic approach to investigate their chemistry, biosynthesis, distribution, and effect on human health. *Antioxidants*, **10**, 1229.

Mohammadparast, B., **Rasouli, M.** & **Eyni, M.** (2024) Resveratrol contents of 27 grape cultivars. *Applied Fruit Science*, **66**, 1–8.

Najafi, S., **Bertini, E.**, **D'Incà, E.**, **Fasoli, M.** & **Zenoni, S.** (2023) DNA-free genome editing in grapevine using CRISPR/Cas9 ribonucleoprotein complexes followed by protoplast regeneration. *Horticulture Research*, **10**, uhac240.

Nerva, L., **Dalla Costa, L.**, **Ciacciulli, A.**, **Sabbadini, S.**, **Pavese, V.**, **Dondini, L.** ***et al.*** (2023) The role of Italy in the use of advanced plant genomic techniques on fruit trees: state of the art and future perspectives. *International Journal of Molecular Sciences*, **24**, 977.

Nerva, L., **Garcia, J.F.**, **Favaretto, F.**, **Giudice, G.**, **Moffa, L.**, **Sandrini, M.** ***et al.*** (2022) The hidden world within plants: metatranscriptomics unveils

the complexity of wood microbiomes. *Journal of Experimental Botany*, **73**, 2682–2697.

Nerva, L., **Moffa, L.**, **Giudice, G.**, **Giorgianni, A.**, **Tomasi, D.** & **Chitarra, W.** (2021) Microscale analysis of soil characteristics and microbiomes reveals potential impacts on plants and fruit: vineyard as a model case study. *Plant and Soil*, **462**, 525–541.

Neuefeind, T., **Reinemer, P.** & **Bieseler, B.** (1997) Plant *glutathione S-transferases* and herbicide detoxification. *Biological Chemistry*, **378**, 199–205.

Nuzzo, F., **Gambino, G.** & **Perrone, I.** (2022) Unlocking grapevine in vitro regeneration: issues and perspectives for genetic improvement and functional genomic studies. *Plant Physiology and Biochemistry*, **193**, 99–109.

Olivares, F., **Loyola, R.**, **Olmedo, B.**, **Miccono, M.Á.**, **Aguirre, C.**, **Vergara, R.** ***et al.*** (2021) CRISPR/Cas9 targeted editing of genes associated with fungal susceptibility *in Vitis vinifera* L. cv. Thompson seedless using Geminivirus-derived replicons. *Frontiers in Plant Science*, **12**, 791030.

Peng, Y., **Yang, J.**, **Li, X.** & **Zhang, Y.** (2021) Salicylic acid: biosynthesis and signaling. *Annual Review of Plant Biology*, **72**, 761–791.

Pessina, S., **Angeli, D.**, **Martens, S.**, **Visser, R.G.**, **Bai, Y.**, **Salamini, F.** ***et al.*** (2016) The knock-down of the expression of *MdMLO19* reduces susceptibility to powdery mildew (*Podosphaera leucotricha*) in apple (*Malus domestica*). *Plant Biotechnology Journal*, **14**, 2033–2044.

Pessina, S., **Lenzi, L.**, **Perazzolli, M.**, **Campa, M.**, **Dalla Costa, L.**, **Urso, S.** ***et al.*** (2016) Knockdown of *MLO* genes reduces susceptibility to powdery mildew in grapevine. *Horticulture Research*, **3**, 16016.

Piffanelli, P., **Zhou, F.**, **Casais, C.**, **Orme, J.**, **Jarosch, B.**, **Schaffrath, U.** ***et al.*** (2002) The barley *MLO* modulator of defense and cell death is responsive to biotic and abiotic stress stimuli. *Plant Physiology*, **129**, 1076–1085.

Probst, C.M., **Ridgway, H.J.**, **Jaspers, M.V.** & **Eirian Jones, E.** (2019) Pathogenicity of *Ilyonectria liriodendri* and *Dactylonectria macrodidyma* propagules in grapevines. *European Journal of Plant Pathology*, **154**, 405–421.

Reddy, V.S., **Ali, G.S.** & **Reddy, A.** (2003) Characterization of a pathogen-induced calmodulin-binding protein: mapping of four Ca^{2+}-dependent calmodulin-binding domains. *Plant Molecular Biology*, **52**, 143–159.

van Schie, C.C. & **Takken, F.L.** (2014) Susceptibility genes 101: how to be a good host. *Annual Review of Phytopathology*, **52**, 551–581.

Schnee, S., **Viret, O.** & **Gindro, K.** (2008) Role of stilbenes in the resistance of grapevine to powdery mildew. *Physiological and Molecular Plant Pathology*, **72**, 128–133.

Scintilla, S., **Salvagnin, U.**, **Giacomelli, L.**, **Zeilmaker, T.**, **Malnoy, M.A.**, **Rouppe van der Voort, J.** ***et al.*** (2022) Regeneration of non-chimeric plants from DNA-free edited grapevine protoplasts. *Frontiers in Plant Science*, **13**, 1078931.

Sheridan, C. (2024) A second chance for plant biotechnology in Europe. *Nature Biotechnology*, **42**, 687–689.

Shi, X., **Cao, S.**, **Wang, X.**, **Huang, S.**, **Wang, Y.**, **Liu, Z.** ***et al.*** (2023) The complete reference genome for grapevine (*Vitis vinifera* L.) genetics and breeding. *Horticulture Research*, **10**, uhad061.

Shi, Z., **Maximova, S.**, **Liu, Y.**, **Verica, J.** & **Guiltinan, M.J.** (2013) The salicylic acid receptor NPR3 is a negative regulator of the transcriptional defense response during early flower development in *Arabidopsis*. *Molecular Plant*, **6**, 802–816.

Singh, B.K., **Delgado-Baquerizo, M.**, **Egidi, E.**, **Guirado, E.**, **Leach, J.E.**, **Liu, H.** ***et al.*** (2023) Climate change impacts on plant pathogens, food security and paths forward. *Nature Reviews Microbiology*, **21**, 640–656.

Singleton, V.L. (1966) The total phenolic content of grape berries during the maturation of several varieties. *American Journal of Enology and Viticulture*, **17**, 126–134.

Sun, B., **Ribes, A.M.**, **Leandro, M.C.**, **Belchior, A.P.** & **Spranger, M.I.** (2006) Stilbenes: quantitative extraction from grape skins, contribution of grape solids to wine and variation during wine maturation. *Analytica Chimica Acta*, **563**, 382–390.

Sung, Y.-C., **Lin, C.-P.**, **Hsu, H.-J.**, **Chen, Y.-L.** & **Chen, J.-C.** (2019) Silencing of *CrNPR1* and *CrNPR3* alters plant susceptibility to periwinkle leaf yellowing phytoplasma. *Frontiers in Plant Science*, **10**, 471737.

Tang, K., **Zhan, J.-C.**, **Yang, H.-R.** & **Huang, W.-D.** (2010) Changes of resveratrol and antioxidant enzymes during UV-induced plant defense response in peanut seedlings. *Journal of Plant Physiology*, **167**, 95–102.

Torregrosa, L., **Vialet, S.**, **Adivèze, A.**, **Iocco-Corena, P.** & **Thomas, M.R.** (2015) Grapevine (*Vitis vinifera* L.). *Agrobacterium Protocols*, **2**, 177–194.

Tricoli, D.M. & **Debernardi, J.M.** (2024) An efficient protoplast-based genome editing protocol for *Vitis* species. *Horticulture Research*, **11**, uhad266.

Trifinopoulos, J., **Nguyen, L.-T.**, **Haeseler, A.v.** & **Minh, B.Q.** (2016) W-IQ-TREE: a fast online phylogenetic tool for maximum likelihood analysis. *Nucleic Acids Research*, **44**, W232–W235.

Trouvelot, S., **Héloir, M.-C.**, **Poinssot, B.** ***et al.*** (2014) Carbohydrates in plant immunity and plant protection: roles and potential application as foliar sprays. *Frontiers in Plant Science*, **5**, 592.

Valtaud, C., **Foyer, C.H.**, **Fleurat-Lessard, P.** & **Bourbouloux, A.** (2009) Systemic effects on leaf glutathione metabolism and defence protein expression caused by esca infection in grapevines. *Functional Plant Biology*, **36**, 260–279.

Velasco, R., **Zharkikh, A.**, **Troggio, M.**, **Cartwright, D.A.**, **Cestaro, A.**, **Pruss, D.** ***et al.*** (2007) A high quality draft consensus sequence of the genome of a heterozygous grapevine variety. *PLoS One*, **2**, e1326.

Viret, O., **Spring, J.-L.** & **Gindro, K.** (2018) Stilbenes: biomarkers of grapevine resistance to fungal diseases. *OENO one*, **52**, 235–241.

Vlot, A.C., **Sales, J.H.**, **Lenk, M.**, **Bauer, K.**, **Brambilla, A.**, **Sommer, A.** ***et al.*** (2021) Systemic propagation of immunity in plants. *New Phytologist*, **229**, 1234–1250.

Wan, D.-Y., **Guo, Y.**, **Cheng, Y.**, **Hu, Y.**, **Xiao, S.**, **Wang, Y.** ***et al.*** (2020) CRISPR/Cas9-mediated mutagenesis of *VvMLO3* results in enhanced resistance to powdery mildew in grapevine (*Vitis vinifera*). *Horticulture Research*, **7**, 116.

Wang, W., **Withers, J.**, **Li, H.**, **Zwack, P.J.**, **Rusnac, D.V.**, **Shi, H.** ***et al.*** (2020) Structural basis of salicylic acid perception by *Arabidopsis* NPR proteins. *Nature*, **586**, 311–316.

Wang, X., **Tu, M.**, **Wang, Y.**, **Zhang, Y.**, **Yin, W.**, **Fang, J.** ***et al.*** (2024) Telomere-to-telomere and gap-free genome assembly of a susceptible grapevine species (Thompson seedless) to facilitate grape functional genomics. *Horticulture Research*, **11**, uhad260.

Wang, Y., **Chen, B.**, **Hu, Y.**, **Li, J.** & **Lin, Z.** (2005) Inducible excision of selectable marker gene from transgenic plants by the Cre/lox site-specific recombination system. *Transgenic Research*, **14**, 605–614.

Wolter, M., **Hollricher, K.**, **Salamini, F.** & **Schulze-Lefert, P.** (1993) The *mlo* resistance alleles to powdery mildew infection in barley trigger a developmentally controlled defence mimic phenotype. *Molecular and General Genetics MGG*, **239**, 122–128.

Wu, Y., **Zhang, D.**, **Chu, J.Y.**, **Boyle, P.**, **Wang, Y.**, **Brindle, I.D.** ***et al.*** (2012) The Arabidopsis NPR1 protein is a receptor for the plant defense hormone salicylic acid. *Cell Reports*, **1**, 639–647.

Ye, X., **Vaghchhipawala, Z.**, **Williams, E.J.**, **Fu, C.**, **Liu, J.**, **Lu, F.** ***et al.*** (2023) Cre-mediated autoexcision of selectable marker genes in soybean, cotton, canola and maize transgenic plants. *Plant Cell Reports*, **42**, 45–55.

Yuan, M., **Ngou, B.P.M.**, **Ding, P.** & **Xin, X.-F.** (2021) PTI-ETI crosstalk: an integrative view of plant immunity. *Current Opinion in Plant Biology*, **62**, 102030.

Zaidi, S.S.-A., **Mukhtar, M.S.** & **Mansoor, S.** (2018) Genome editing: targeting susceptibility genes for plant disease resistance. *Trends in Biotechnology*, **36**, 898–906.

Zhan, X., **Lu, Y.**, **Zhu, J.** & **Botella, J.R.** (2021) Genome editing for plant research and crop improvement. *Journal of Integrative Plant Biology*, **63**, 3–33.

Zheng, Z., **Nonomura, T.**, **Appiano, M.**, **Pavan, S.**, **Matsuda, Y.**, **Toyoda, H.** ***et al.*** (2013) Loss of function in *Mlo* orthologs reduces susceptibility of pepper and tomato to powdery mildew disease caused by *Leveillula taurica*. *PLoS One*, **8**, e70723.

Zhou, P., **Zavaliev, R.**, **Xiang, Y.** & **Dong, X.** (2023) Seeing is believing: understanding functions of *NPR1* and its paralogs in plant immunity through cellular and structural analyses. *Current Opinion in Plant Biology*, **73**, 102352.

Zhu, H., **Li, C.** & **Gao, C.** (2020) Applications of CRISPR–Cas in agriculture and plant biotechnology. *Nature Reviews Molecular Cell Biology*, **21**, 661–677.

Zuo, J., **Niu, Q.-W.**, **Møller, S.G.** & **Chua, N.-H.** (2001) Chemical-regulated, site-specific DNA excision in transgenic plants. *Nature Biotechnology*, **19**, 157–161.